Politecnico di Torino

Politecnico di Torino

Master's degree in Nanotechnologies for ICTs

Thesis title :-

FLEXIBLE AND WEARABLE INTEGRATED DEVICES FOR ENERGY HARVESTING AND STORAGE, EMPLOYING ADVANCED SOLAR CELLS (dye sensitized and perovskites) AND SUPERCAPACITORS

Supervisors: Professor Elena Tresso

Author…Muluken Animaw Sinishaw…….s226346

Index: -
Pages

Abstract

Flexible devices have demonstrated great potential in a wide range of applications including wearable devices for fitness and health care. Flexible plastic substrates, such as polyimide, or transparent conductive polyester are used to fabricate flexible devices that increase the comfort when they are worn by users or patients. Flexible fiber solar cells are wire-shaped solar cells fabricated on wire-like substrates. These devices, including inorganic, organic, dye-sensitized and perovskite solar cells have made great progress in the recent years. In the case of flexible dye-sensitized solar cells the energy conversion efficiency has increased up to 3.38 %

Wearable devices are electronic products that are applied for worn on the human body sensing, artificial skins, wearable communication, monitor the health of patients and entertainment. They are controlled by electronic components and software. Nowadays, a variety of wearable and portable devices, such as smart glasses and smartwatches, have been invented. The demand of these electronics has been growing steadily. These wearable devices need energy for their operating system. Some parts of wearable devices like the electrodes and other internal parts must be mechanically strong, flexible, lightweight, and comfortable to the user.

Supercapacitors are energy storage devices which provide high power densities and long cyclic life compared to other storage devices (e.g., Li-ion, lead acid and alkaline batteries). These capacitors mainly use high dielectric materials to store more energy in a shorter time .Flexible supercapacitors (SCs) have attracted widespread interest in developing lightweight, thin, elastic and efficient portable/wearable energy storage devices that show promising

applications in hybrid electric vehicles, uninterruptible power supplies and “smart textiles”.

1. INTRODUCTION

The world total primary energy supply is increasing by double from years 1973 to 2015 as the international energy agency reports. For developing countries the consumption will increase in the next future in order to quickly get a development from the industry.

One of the most promising renewable and “green” energy is solar energy.

In particular, devices which can provide both the harvesting and the storage of energy play a vital role in human daily life due to the possibility of replacing conventional energy from fossil fuels. These devices include lithium-ion batteries (LIBs), supercapacitors (SCs), nanogenerators (NGs), biofuel cells (BFCs), photodetectors (PDs), and solar cells. However, these isolated devices only have limited performance and cannot provide enough energy for applications with long-term run. Integrated energy harvesting-storage devices that include photo charging devices for the functions of photo electric energy conversion like dye sensitized, perovskites solar cells, etc and electrochemical energy storage like supercapacitors, attracted enormous attention to serve as sustainable and portable distributed power sources. Developing integrated power pack, combining energy harvesting and storage, is an effective path to obtain a small size, light weight, high density and high reliability energy system.

2. DYE SENSITIZED SOLAR CELLS (DSC)

A dye-sensitized solar cell (or Grätzel cell) is a low-cost solar cell based on a photo electrochemical system, formed by a photo sensitized anode, an electrolyte and a counter-electrode. The DSSC has a number of attractive features; it is simple to make using conventional roll-printing techniques. It is semi-flexible and semi-transparent which offers a variety of uses not applicable to glass-based systems and most of the materials used are low-cost.

Researchers are developing the electrical properties and performance of DSSC by inserting suitable materials into TiO2 film. For example Fe_3O_4 has attained attention of researchers to modify the optoelectronic devices in the field of biomedical and as a photocatalyst because of its high specific surface area, biocompatibility and good dispersion.

Recently written literature reports that fully organic dyes with various structures got highest efficiency of 14.3% by replacing metal by organic dyes.

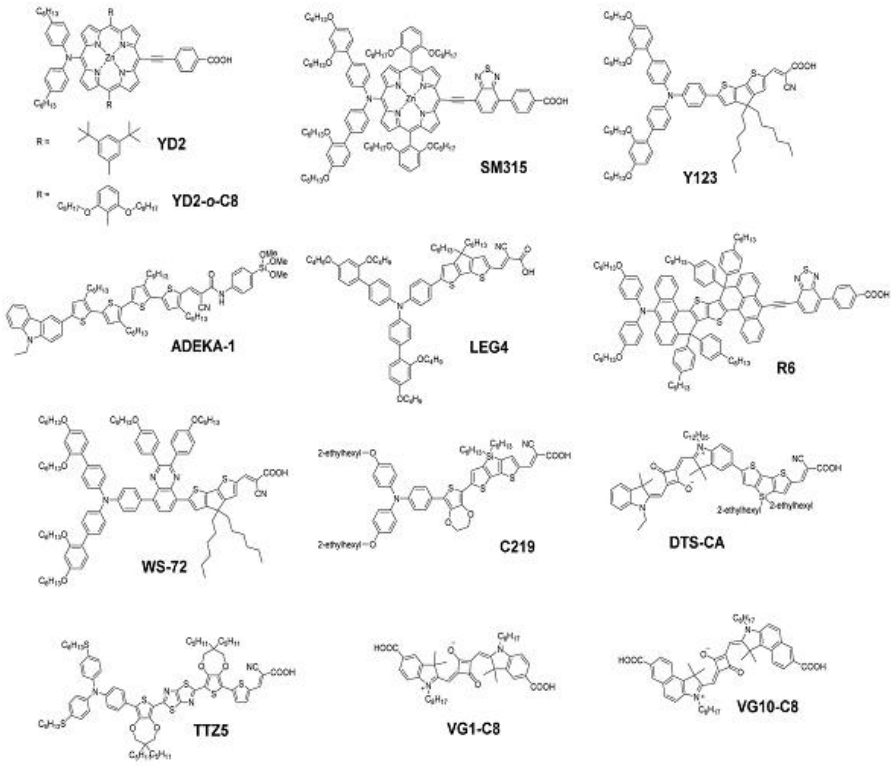

The above figure shows structures of various photosensitizers: porphyrins (YD2 and YD2-o-C8) and fully organic dyes. [Reference 1]

From the above figure of molecular dye structure that shows good performance porphyrin dyes is the YD-2 dye. In 2011 , Yella et al. planned a tailored variant of YD-2 which has the donor–π-acceptor (D–π-A) Zn porphyrin dye YD2-o-C8 and got a power conversion efficiency of 11.9% by using a cobalt(II/III) tris(bipyridyl)-based redox electrolyte, with a VOC of 965 mV and JSC of 17.3 mA cm^{-2} under standard air mass (AM) 1.5 sunlight at 995 W m^{-2}

intensity. In this configuration YD2-o-C8 absorbs light over the whole VIS range and bears two octyloxy groups in the ortho positions of each meso-phenyl ring . Moreover, by using simulated AM1.5G sun light, this porphyrin dye reached a power conversion efficiency (PCE) of 12.3% when co-sensitized with the Y123 organic D–π-A dye. Further in 2014 Mathewet al proposed tailored modification on the zinc-porphyrin structure which include bulky bis(2',4'-bis(hexyloxy)-[1,1'-biphenyl]-4-yl)amine donor group and proposed a novel benzothiadiazole group as an acceptor. The panchromatic porphyrin sensitizer SM315 in the above figure, together with a $[Co(bpy)_3]^{2+/3+}$redox couple, resulted an improved JSC (18.1 mA cm^{-2}) with a record 13.0% power conversion efficiency at full sun illumination without the need for a co-sensitizer. The other novel result is metal-free sensitizing dye , ADEKA-1 (a carbazole/alkyl-functionalized oligothiophene with an alkoxysi-lyl-anchor moiety resulted improved light-to-electric energy conversion efficiencies of over 12% . With the same dye given a result of 14% PCE in the presence of the co-sensitizer LEG4 (a carboxy-anchor organic sensitizing dye) . In more detail is found in the table which describes efficiency comparison of different materials .

2.1. The basic concepts

Dye-sensitized solar cells(DSSCs) are electrochemical cells based on the idea of using the reactions of photosynthesis to convert sun light in to electrical power . When a DSSC is getting sun light , then the electromagnetic radiation passes in to the transparent glass of the photo anode and reach the semiconductor layer that contain dye molecules .The electromagnetic radiation which is absorbed by the dye molecules which depends its absorption spectrum turns into an excited state that indicates an electron from the highest occupied molecular orbital (HOMO) to the lowest unoccupied molecular orbital (LUMO) or according to energy level LUMO has higher energy level with respect to the conduction band of the dye-hosting semiconductor. Then electrons pass through mesoporus structure to reach the conductive glass. After electons pass through the external circuit , they arrive counter electrode . The counter electrode is the

other part of DSSC in which reduction of tri-iodide to iodide takes place. Ions that diffuse from the electrolyte migrate to the circuit. The amount of dye molecules adsorbed on its surface depends on the dominant factors which are the porosity and morphology of the semiconductor layer. For higher surface areas, it is good for large reaction site to harvest the incident light.

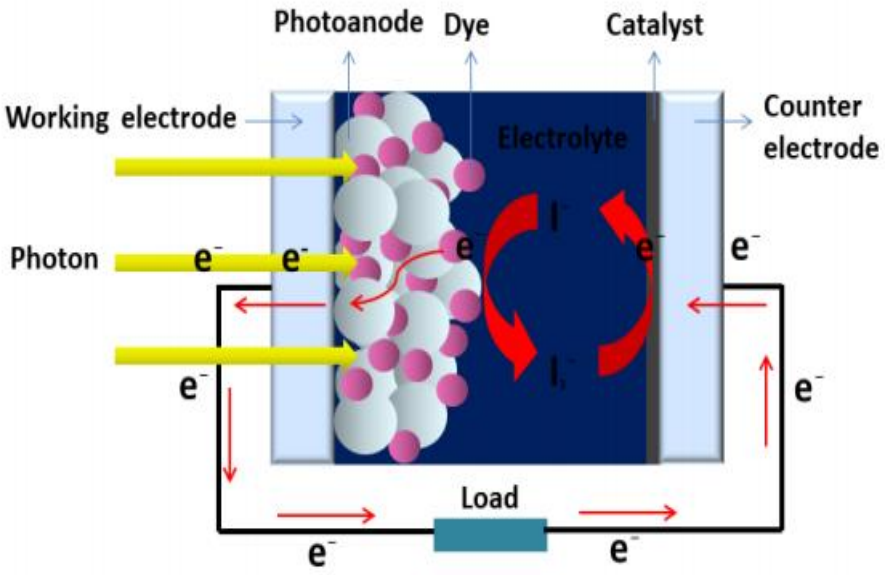

Figure 2.1: Structure of a DSSC [Reference 2]

2.2. The different elements of a DSC

Dye-sensitized solar cells(DSSCs)cells are belonging to the emerging third-generation photovoltaic concept and use synthetic or natural dyes as light harvesting pigments .The different parts of a DSC are the following

1. A photo anode, in most cases transparent glass covered with a transparent conductive oxide (TCO) material usually indium tin oxide (ITO) or fluorine doped tin oxide (FTO) is used. The anode is soaked with a dye solution which bonds to the TiO2. To absorb electromagnetic radiation coming from the sun, the dye molecules attached on to the high surface area of the semiconductor part.

2. An electrolyte :- A widely used liquid electrolyte is the iodide–triiodide (I^-/I^{-3}) redox system in an organic solvent which penetrates into the nano porous structure.
3. A counter electrode which has a place for a nanometric pt electrode is deposited which act as a catalyst inside the electrolyte for reduction reaction process.

2.3. The principal characterization methods (I -V curves, Quantum efficiency, EIS, …)

a. I -V curves

All photovoltaics, including DSSCs, must have a modular structure where several cells are connected in series for obtaining sufficiently high voltage for applications. However, the performances of the individual cells in the module are not always uniform because it may be affected by shadows, clouds and dirt when installed outdoors. In particular, the outputs of the cells in the modules of DSSCs are often non-uniform because of the market demands for multi colour and transparent cells. In the figure below Fig. 2.3 (a) shows three types of typical DSSC current–voltage (*I*–*V*) characteristics for the same size of photodetector but the different colors and transmittance of photodetector due to sensitizers and thickness of photodetector layers. Fig 2.3(b) shows the *I*–*V* characteristics of a module comprising the cells shown in Fig .2.3(a) connected in series. Fig. 2.3(a) indicates that the difference in DSSC components has a larger influence on short-circuit currents than on open-circuit voltages or fill factors. Fig. 2.3(b) shows that the *I*–*V* characteristics of series-connected cells with different short-circuit currents shape the step-like curve. When the module generates electrical power on the operating point A in Fig.2.3(b) , all individual cells are operated in the first quadrant via the power control circuit for photovoltaic generation. In contrast, when the module generates electrical power on the operating point B in Fig.2.3(b) , Cell-1 and Cell-2 are operated in the first quadrant, whereas Cell-3, which has the lowest short-circuit current, is operated in the second quadrant. In this case, a reverse voltage is applied to Cell-3 (as opposed to a forward voltage).

When the reverse voltage reaches 1500 mV, the dye and electrolyte components of DSSCs have been reported to decompose. The current characteristics of DSSCs shown in the second quadrant of Fig.2.3(a) are important in preventing the application of excessive reverse voltages to cells in series.

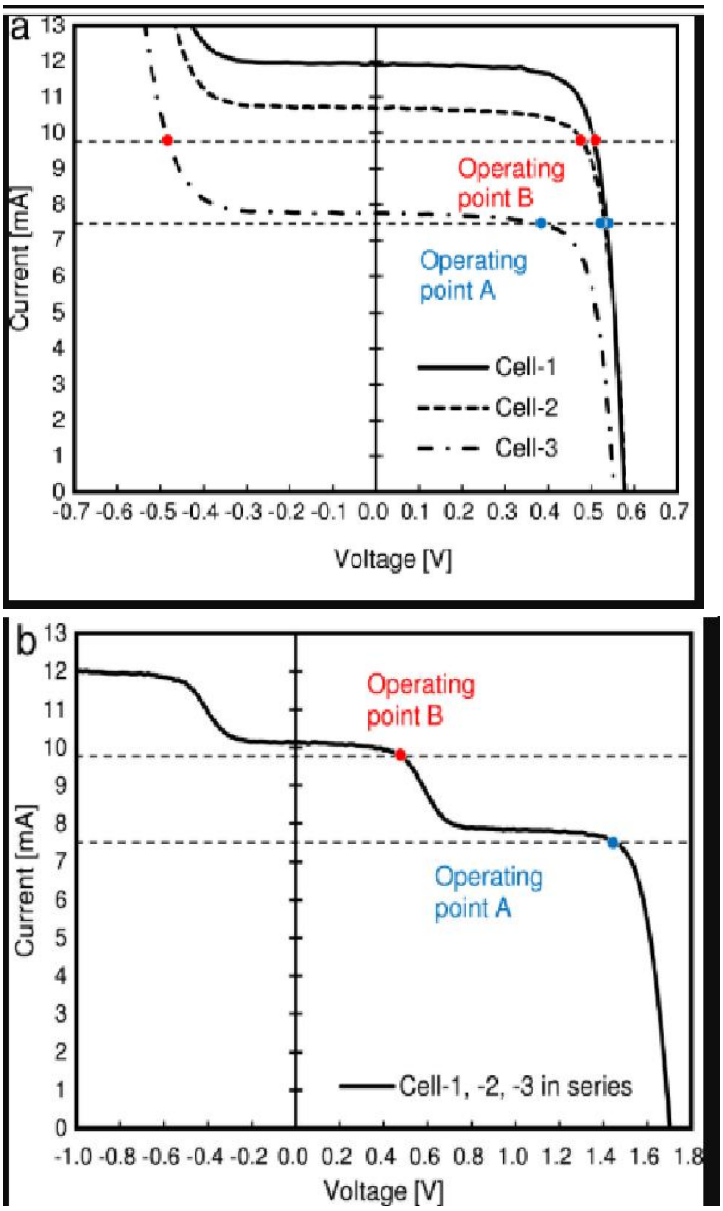

Fig. 2.3. a Typical current–voltage (*I–V*) characteristics under standard air mass 1.5 (AM 1.5) solar spectrum light: (a) cells with different compositions and (b) a module comprising the serial connection of the cells shown in (a). [Reference 3]

b. Quantum efficiency

Two types of quantum efficiency of a solar cell are often considered:

- External Quantum Efficiency (EQE) is the ratio of the number of charge carriers collected by the solar cell to the number of photons of a given energy shining on the solar cell from outside (incident photons).
- Internal Quantum Efficiency (IQE) is the ratio of the number of charge carriers collected by the solar cell to the number of photons of a given energy that shine on the solar cell from outside and are absorbed by the cell.

The IQE is always larger than the EQE. A low IQE indicates that the active layer of the solar cell is unable to make good use of the photons. To measure the IQE, one first measures the EQE of the solar device, then measures its transmission and reflection, and combines these data to infer the IQE.

$$\mathrm{EQE} = \frac{\text{electrons/sec}}{\text{photons/sec}} = \frac{\text{(current)/(charge of one electron)}}{\text{(total power of photons)/(energy of one photon)}}$$

$$\mathrm{IQE} = \frac{\text{electrons/sec}}{\text{absorbed photons/sec}} = \frac{\mathrm{EQE}}{\text{1-Reflection-Transmission}}$$

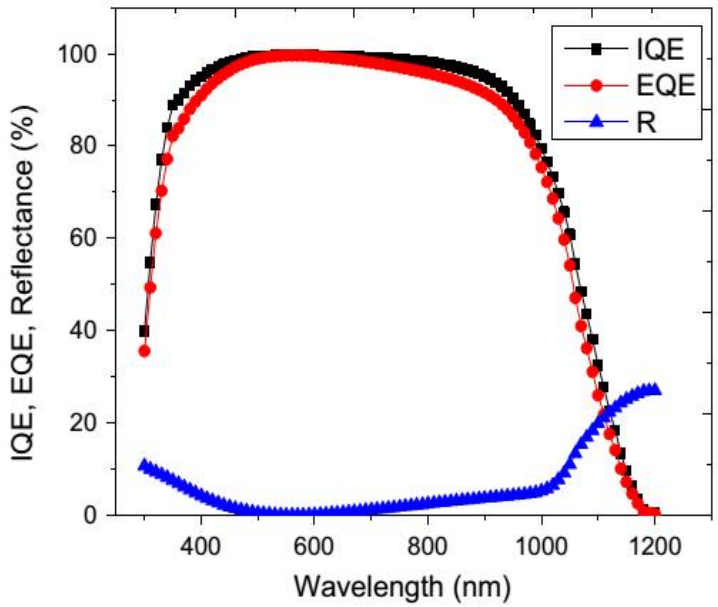

Figure 2.3.b. Internal quantum efficiency (IQE), external quantum efficiency (EQE), and front surface reflection (R) of the solar cell devices [Reference 4]

Currently the best efficiency value reported for DSSCs research is 14.3%. In the figure below the DSSC efficiency shows a quite slow constant increment during some years .

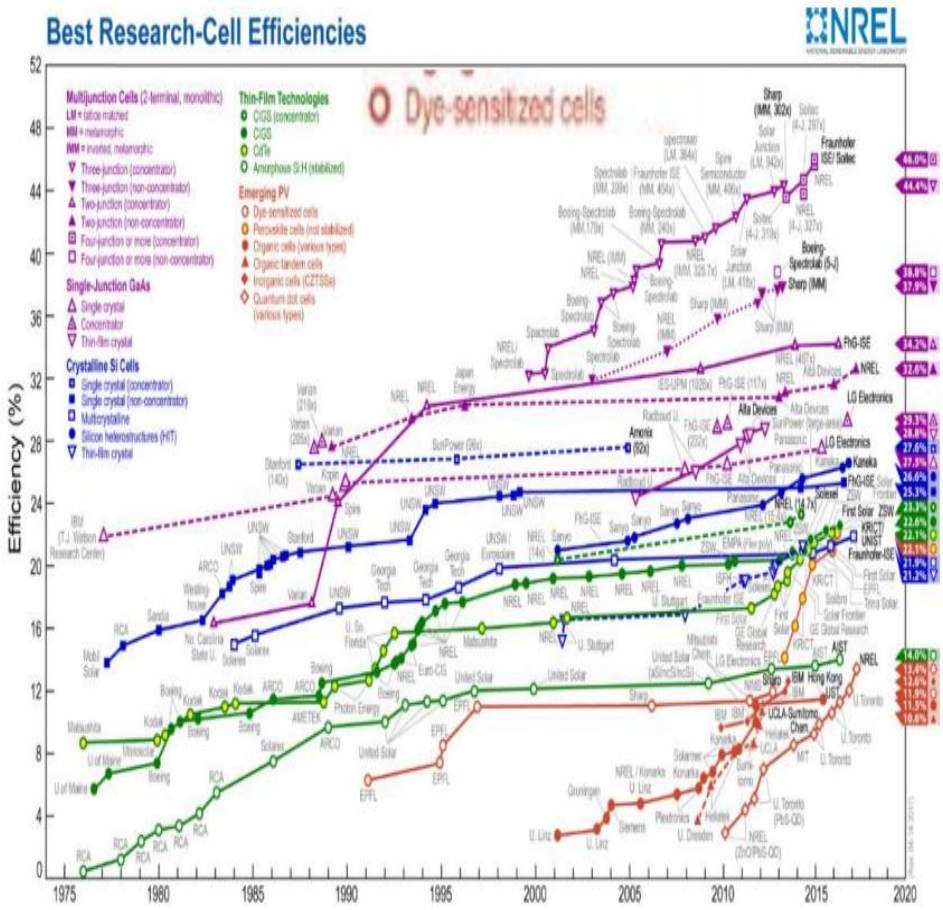

Figure 2.3.c Best research-cell efficiencies graph. Efficiencies are reported as a function of the PV cell fabrication year. [Reference 5]

Here is another efficiency comparison with different Photosensitizers for DSSCs [Reference 1]

Class	Dye	properties	Issues	η(%)
Zn-Porphyrin	YD2	• Iodide/triiodide electrolyte • Broad absorption	• Not meaningful	11.1
	YD2-o-C8	• High PCE • High stability	• Cobalt-based electrolyte: Co $(bpy)_3^{3+/2+}$	11.9
	YD2-o-C8 + Y123	• High PCE • High stability	• Cobalt-based electrolyte: Co $(bpy)_3^{3+/2+}$	12.3
	SM315	• Panchromatic absorption • No need of co-sensitization • Very high PCE	• Cobalt-based electrolyte: Co $(bpy)_3^{3+/2+}$	13.0
D–π-A	Adeka-1	• High PCE • High stability	• $[Co(Cl\text{-}phen)_3]^{3+/2+}$	12.5
	Adeka-1 + LEG4	• Iodide/triiodide electrolyte	• Not meaningful	11.2
	Adeka-1 + LEG4	• Record PCE	• Cobalt-based electrolyte: $[Co^{2+}(phen)_3](PF_6^-)_2$	14.3
	R6	• High PCE • High photostability	• Cobalt-based electrolyte: Co $(bpy)_3^{3+/2+}$	12.6
	Y123	• Copper-based electrolyte: Cu $(tmp)_2^{2+/+}$ TFSI	• Not meaningful	13.1
	WS72	• Copper-based electrolyte: Cu $(tmp)_2^{2+/+}$ HTM	• Not meaningful	11.6
	DTS-CA	• Iodide/triiodide electrolyte	• Not meaningful	8.9
Organic squaraine dye	C219	• Iodide/triiodide electrolyte	• Not meaningful	10.1
Flavonoids	Anthocyanin from *M. malabathricum*	• Natural PS • Extended π conjugation	• Low stability • Low PCE	1.1
Carotenoids	MeO-φ-6-CA	• Natural PS	• Low stability • Low PCE	2.6
	PPB + β-carotene	• Natural PS • Iodide/triiodide electrolyte	• Low stability • Co-Sensitization with a chlorophyll derivative • Low PCE	4.2
Chlorophylls	Chlorophyll c1 from *Undaria pinnatifida*	• Natural PS	• Low stability • Low PCE	3.4
	Chlorophyll c2	• Natural PS	• Low stability • Low PCE	4.6
Betalains	SPA	• Natural PS • Iodide/triiodide electrolyte	• Low stability • Low PCE	3.0

c. Electrochemical impedance spectroscopy (EIS)

Electrochemical impedance is usually measured by applying an AC potential (Usually 10 mV) to an electrochemical cell(DSSC, EDLC, battery) and then measuring the current through the cell. The response to this potential is an AC current signal. This current signal can be analysed as a sum of sinusoidal functions.

The impedance of the system calculated as :-

$$Z = \frac{E_t}{I_t} = \frac{E_0 \sin(\omega t)}{I_0 \sin(\omega t + \phi)} = Z_0 \frac{\sin(\omega t)}{\sin(\omega t + \phi)}$$

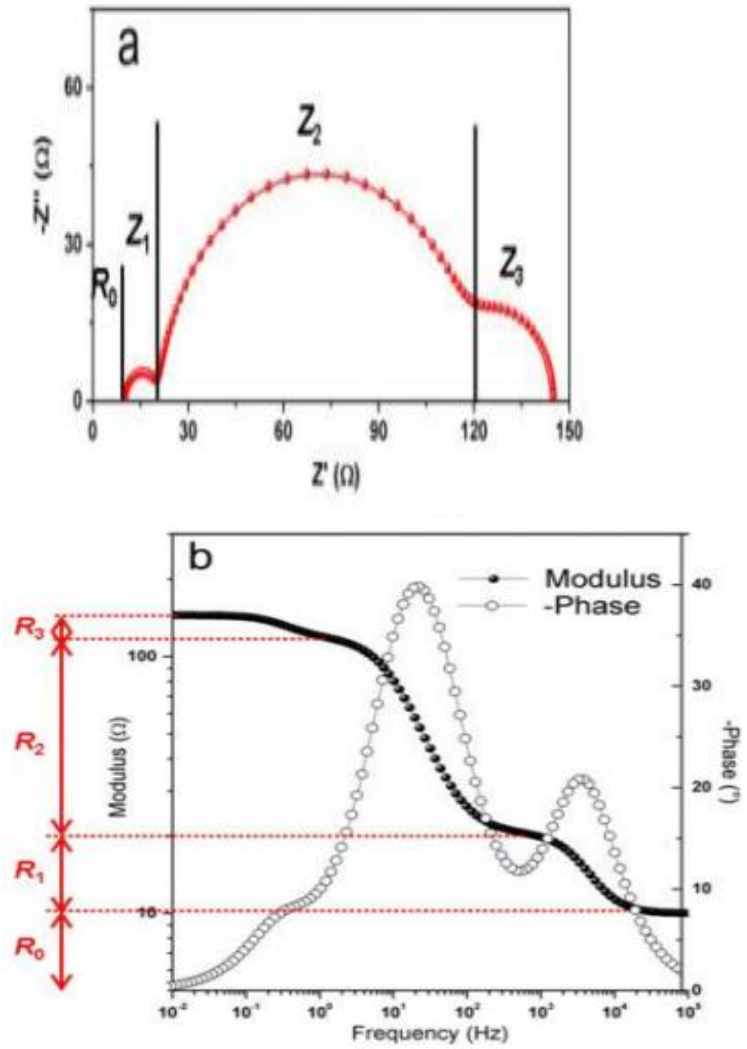

Figure 5: Impedance spectrum of a DSSC measured at open circuit voltage: (a) Nyquist and (b) Bode graphs. [Reference 6]

2.4. Flexible DSC

Flexible solar cells have attracted tremendous interest

Flexible solar cells have attracted tremendous interest because of its potential for wearable electronics and other versatile applications. DSSCs solar are

commonly fabricated on to planar conductive glass substrates and the glass based architecture has some critical constraints like rigidity, frangibility and weight. For the construction of large part of glass based DSSC, expensive conductive glasses used. Typically, the photoanodes of flexible DSSCs consist of titanium oxide nanocrystals on a plastic substrate that are produced by utilizing low temperature processes such as sintering, mechanical pressing, hydrothermal crystallization, electrophoretic deposition, microwave irradiation, or film transfer. It is expected that decreasing temperature process leads to lower efficiencies due to this reason alternative treatments should be used . Applying metallic substrate at the anode results in high temperature sintering but due to metallic substrate its opaque it leads unavoidable a backward cell irradiation. So the solution for this problem is by using a transparent electrolyte that increase 10% of the short circuit current density which is experienced with a deposition of submicron Sio2 transparent beads onto the TiO2 layer . So transparent beads occupied a fraction of the opaque electrolyte and enhanced the number of photons which could reach the hosting dye mesoporous layer, improving the overall transmittance of the electrolyte chamber.

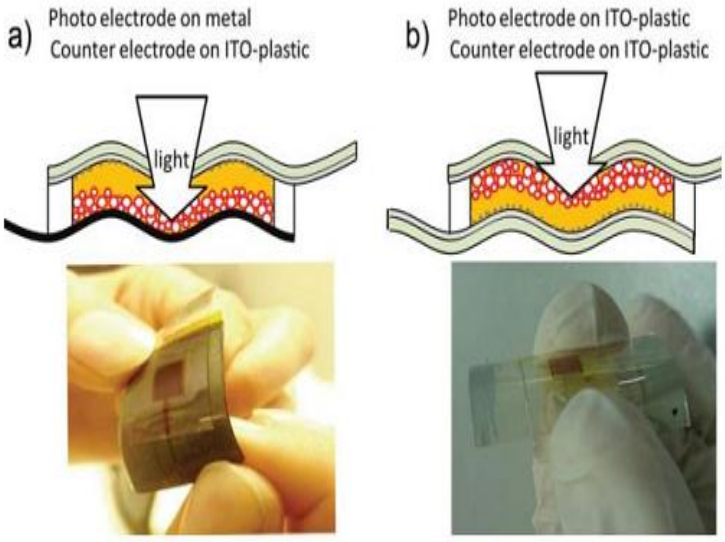

Figure 2.4 Literature widespread flexible DSSC architectures, presenting a backward illumination (metallic substrate at the photo-anode) a) or a forward

illumination (plastic substrates both for the anode and cathode) b [Reference 5]

Recent researches reported that for the construction of flexible dye-sensitized solar cells (DSSCs), developing flexible counter electrode (CE) and Photoanode are the main part that should be considered . To get the flexible CE , carbon nanotubes (CNTs) are applied for the modification of flexible TiO2/C nanofibrous film. So this CNTs/TiO2/C conjugation results a good flexibility .In general a perfect flexible CE contains electro-catalytic activity towards the redox couple in electrolyte with well combination between the electrocatalytic material and flexible substrate. Here platinum (Pt) is used to prepare flexible CE due to its excellent electro-catalytic activity .

2.4.1 Preparation of the CNTs/TiO2/C nanofibrous film

The fabrication of CNTs/TiO2/C started using electrospinning technique followed by heat treatment that is 0.4 g polyvinylpyrrolidone (PVP, 1,300,000), 0.4 g polyacrylonitrile (PAN, Mw = 140,000), 0.5 mL acetic acid, 0.7 g titanium (IV) isopropoxide (TiP, 97%, Aldrich), and a certain amount of multi-walled carbon nanotubes (MWCNTs) were dissolved in 6 mL of N,N-dimethyl formamide (DMF, 99.5%, Aladdin), and then they were stirred constantly for 8 h and ultrasonic treated for 2 h to form different electrospinning solutions. After this process each electrospinning solution was electro spun on a grounded collector with the flow rate of 0.9 mL/h, the electric voltage of 15 kV and the collector distance of 12 cm. In this step the precursor nanofibrous films achieved . After this all the precursor nanofibrous films were thermally stabilized in a tube furnace at 270 °C in air for 2 h and carbonized at 900 °C under nitrogen for 1 h with a heating rate of 2 °C/min.

By using some precent contents of CNTs 0%, 0.5%, 1%, 2% and 3% , the different CNTs/TiO2/C nanofibrous films were obtained.

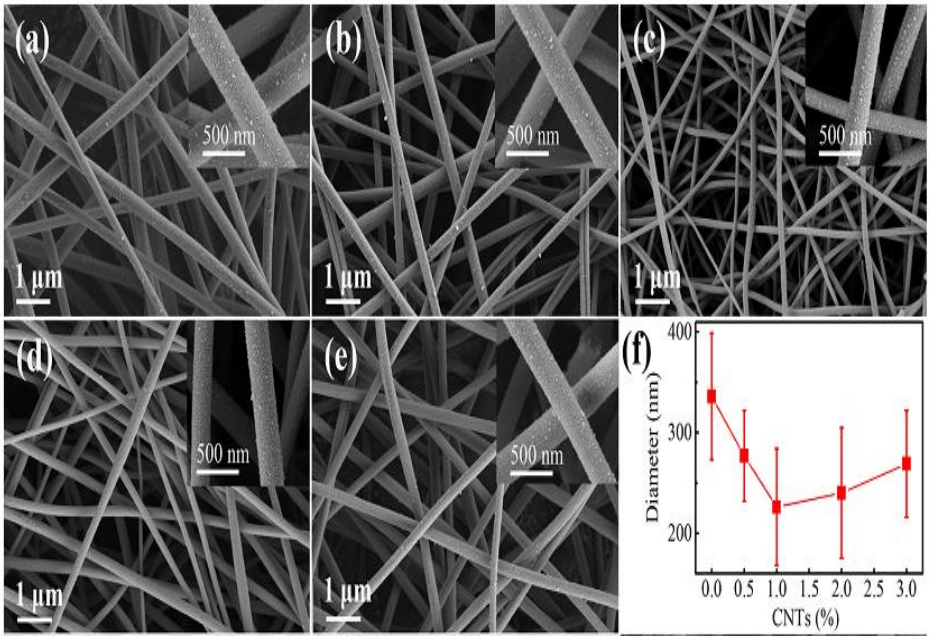

The above fig. shows that FESEM images of the various CNTs/TiO2/C nanofibrous films: 0% (a), 0.5% (b), 1% (c), 2% (d), 3% (e); the average diameters of these NFs (f). [Reference 7]

2.4.2 . Mechanical properties of CNTs/TiO2/C

Some of the mechanical properties of CNTs/TiO2/C were studying from tensile testing and bending (stiffness) testing . Here in the table below summarizes nanofibrous films of the stress-strain cures of the films and the result of bending testing, the initial elastic modulus, strength, elongation at break and elastic modulus of bending . [Reference 7]

Films	Initial elastic modulus (GPa)	Strength (MPa)	Elongation at break (%)	Elastic modulus of Bending (cN/cm^2)
0.0%	1.23	36.15	2.94	7.7
0.5%	1.37	40.08	2.93	7.7
1.0%	1.52	42.15	2.77	8.4
2.0%	1.69	39.44	2.34	9.8
3.0%	1.88	35.29	1.87	13.9

4.2.3 Electrochemical parameters

For the different samples of CNTs 0%, 0.5%, 1%, 2% and 3% , some the research report that there are various CEs and photovoltaic parameters of the flexible DSSCs. Here in the table below some of the electrochemical parameter results are summarized .

Samples	R_s ($\Omega \cdot cm^2$)	R_{ct} ($\Omega \cdot cm^2$)	J_{sc} ($mA \cdot cm^{-2}$)	V_{oc} (V)	FF (%)	η (%)
0.0%	16.64	33.29	9.49	0.681	37.6	2.43
0.5%	16.12	33.13	9.89	0.683	40.1	2.71
1.0%	14.99	33.22	10.21	0.691	40.3	2.84
2.0%	12.25	26.58	10.81	0.710	44.0	3.38
3.0%	13.70	29.16	10.50	0.700	42.2	3.10

Where (Rs) series resistance , (Rct) charge transfer resistance, (Jsc) current density, (Voc) open circuit voltage, (FF) fill factor and efficiency (η) [Reference 7]

2.5. Wearable DSC

Now a days some electronic devices like electronic textile (e-textile) based dye sensitised solar cells wearable technology has been produced for various applications . For example, intelligent biomedical garments for monitoring, diagnosing and treatment of medical conditions, wireless cardiac signal monitoring in sports and military clothing integrating fabric antennas to support networks and communications.

Let us see roughly one application of wearable Dye Sensitized Energy Harvesting which is Flexible Printed Monolithic-Structured Solid-State Dye Sensitized Solar Cells on Woven Glass Fibre Textile for Wearable Energy Harvesting Applications. In recent years the Dye Sensitized is a promising candidate for flexible plastic and e-textile applications because of it's the straightforward and low cost fabrication processes required and high energy conversion efficiency. It is known that the original Dye Sensitized Solar Cell has two rigid glass substrates incorporating the electrodes with a liquid electrolyte injected between them produced by plastic DSSCs using flexible Indium tin oxide/polyethylene naphthalene (ITO/PEN) substrates as front and back electrodes with a liquid electrolyte in-between the sealed plastic substrates which has power conversion efficiency (PCE) of 5.8%. The fabricated DSSCs on a glass fibre textile which had a screen-printed polyamide film to smooth out the textile and a sputtered titanium bottom conductive layer.

Another way of analysing DSSC textiles is to functionalize the yarns and fibres which can be woven in to a textile . Recently Zhang *et al*. explained that a DSSC textiles fabricated using Polybutylene terephthalate (PBT) polymer yarns woven into different fabric structures that used a liquid electrolyte and achieved a PCE of 1.3% for a single fibre which is the highest value for fibre based DSSCs . This approaches have some problem in large area applications to connect a number of crossed, cylindrical yarn solar cells that have been woven into the textiles and the limitation of the bending radius curvature as well as when fibres are tending to break easily which leads degrade in the cell performance. Also when woven into textiles, they are partially shaded which may reduce the power conversion efficiency. Due to conventional liquid electrolyte DSSCs parts of photovoltaic yarns, that suffer from leakage, corrosion and long-term stability problems in practical applications.

To solve these issues hole transport materials or solid electrolyte materials such as the amorphous organic material Spiro-OMeTAD (N^2,N^2,$N^{2'}$,$N^{2'}$,N^7,N^7,$N^{7'}$,$N^{7'}$-octakis(4-methoxyphenyl)-9, 9′-spirobi[fluorene]-2,2′,7,7′-tetraamine) has been used as the most promising solid electrolyte for wearable solid state (ss) DSSCs applications . Hardin *et al*. produces ssDSSC on fluorine doped tin oxide (FTO) glass substrates in which the TiO_2 compact layer (CL) was deposited using spray pyrolysis followed by doctor blading a TiO_2 nanoporous layer for dye sensitisation then spin coating the solid electrolyte spiro-OMeTAD layer . The result of this configuration gives a PCE of 2.7% and 2.8% for the evaporated silver (Ag) and laminated silver nanowire (AgNW) top electrodes respectively. In recent years Margulis *et al*. defined with similar structure of ssDSSCs on FTO glass substrates but after spin coating the solid electrolyte, a PEDOT: PSS layer was spin coated to provide a better contact with the spray coated AgNW top electrode which has an improved PCE of 3.7%. So , to achieve a flexible and stable DSSC on textile a two-dimensional ssDSSC fabricated on woven high temperature (450 °C)glass fibre textile substrates needed.

(a)

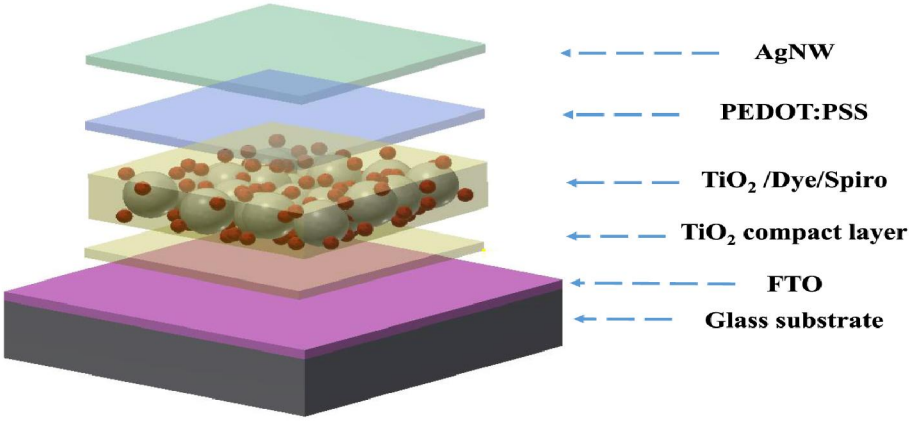
AgNW
PEDOT:PSS
TiO_2 /Dye/Spiro
TiO_2 compact layer
FTO
Glass substrate

(b)

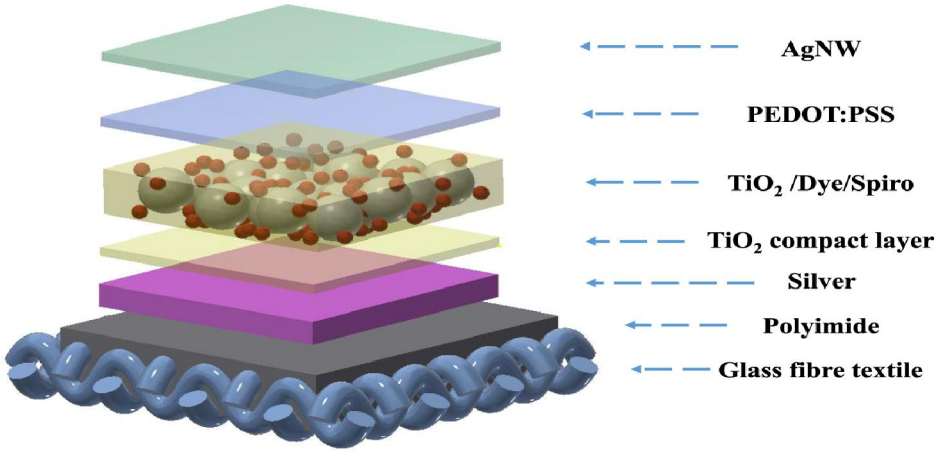
AgNW
PEDOT:PSS
TiO_2 /Dye/Spiro
TiO_2 compact layer
Silver
Polyimide
Glass fibre textile

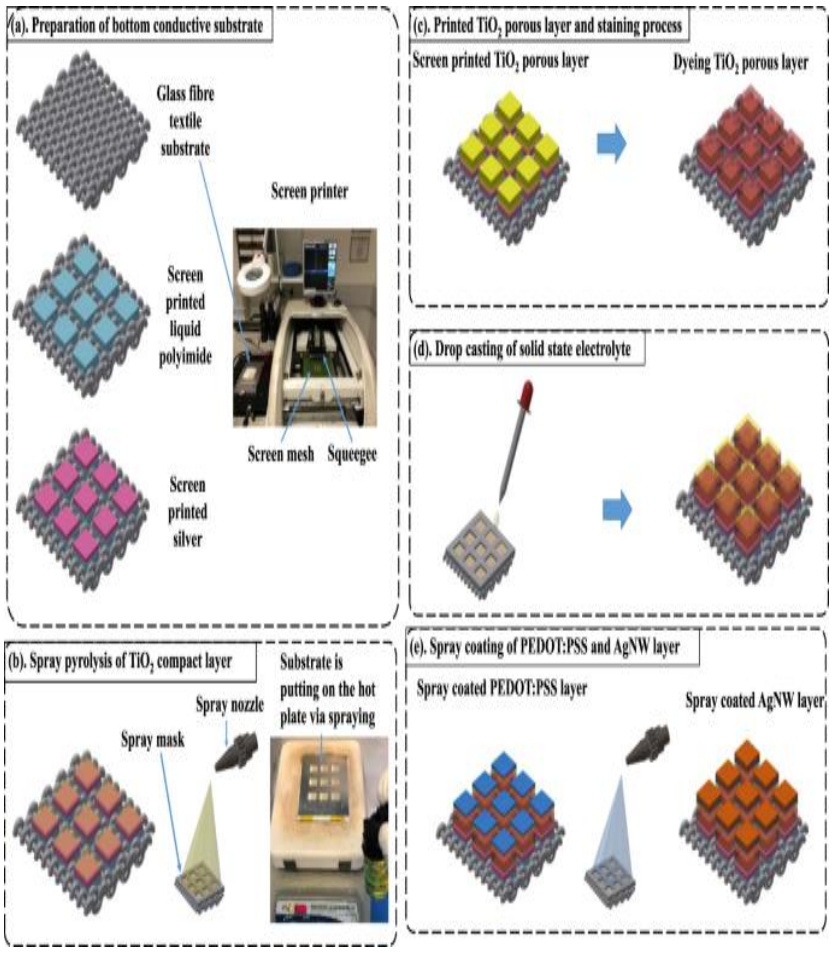

Figure 2.5a

Figure 2.5b

In fig . 2.5a . (a, b) shows that textile based ssDSSC is a flexible 2D planar structure that is a variation of the version fabricated on the glass substrate . All functional layers on both glass and textiles are same, except for the bottom electrode, which is the FTO on glass and a thick film silver layer on the textile substrates . The fabrication process has five steps as shown fig 8(a-e) all functional layers were directly deposited onto the textile substrates using processes such as screen printing and spray coating . To fabricate the ssDSSC, after initial investigations on uncoated textiles, a flexible polyimide layer was required to reduce the surface roughness of fabric. The use of the liquid polyimide to planarise the surface of the fabric is different to the polyurethane based material typically used due to the temperature limitation of the polyurethane film. [Reference 8]

In fig 2.5b shows Fabrication process diagram of textile based ssDSSC, (a) screen printing polyimide and silver layer to form the bottom conductive substrate, (b) spray pyrolysis of TiO_2 compact layer, (c) screen printed TiO_2 porous layer and staining process, (d) drop casting of solid state electrolyte, (3) spray coating of PEDO:PSS and AgNW layer. **[Reference 8]**

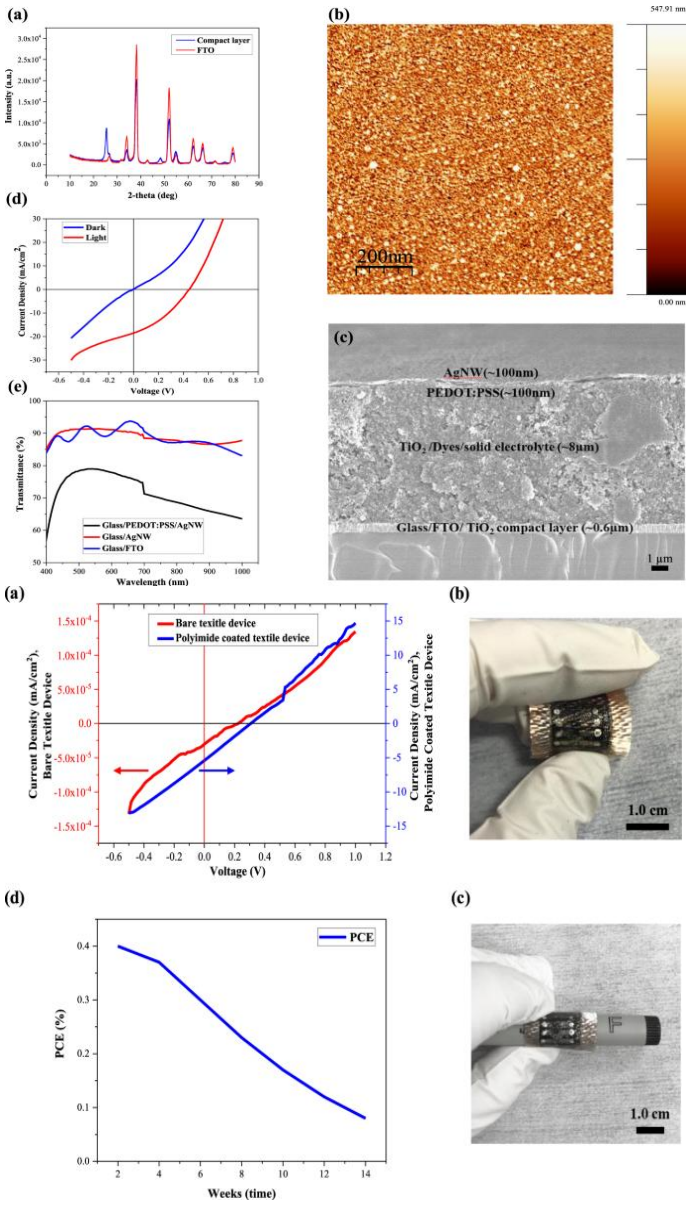

Figure 2.5c

Figure 2.5d

In fig 2.5c. (a-e) shows (a) XRD spectra of the CL TiO_2 film prepared by spray pyrolysis on FTO glass substrate, (b) AFM graph for TiO_2 compact layer (CL) on

FTO glass substrates, (c) FESEM for the cross sectional solid state DSSC device on FTO glass substrates, (d) J/V graph for the FTO glass substrates, and (e) transmission graph for the AgNW and PEDOT:PSS/AgNW glass substrates.

In figure 2.5d . (a-d) shows Photograph of (a) J/V curve of ssDSSCs fabricated on bare glass fibre textiles and polyimide coated glass, (b) Polyimide coated glass fibre textile device under bending, and (c) device rolling on a pen, (d) the PCE versus time regarding stability in air for polyimide coated glass fibre textile. [Reference 8]

Many researchers developed different structures of wearable DSSC by using different materials for the Photoanode and Counter electrode . Finally they got different efficiencies for different assembly . In the table below summarizes comparison of different systems of textile structured solar cells for wearable DSSC. [Reference 9]

Photoanode	Counter electrode	Assembly	Efficiency(%)
Ti metal wires woven with textile yarns	Pt coated Ti metal wires woven with textile yarns	Weaved	0.35%
Titania coated metal wire/Glass fiber yarns	Pt coated metal wire/Glass fiber yarns	interlaced	1.7%
ZnO/ITO	Mo/CIS/CdS	Wire shaped	2.31%
Stainless steel wire coated with TiO_2/PCBM	Metal wire	Wire shaped	3.87%
TiO_2/Stain less steel metal mesh (SUS 304)	Pt coated carbon on stain less steel (SUS 304)	Stacked	4.17%
Ti wires	Carbon nanotube fibers	Stacked	3.67%
Polyester/Ag-NW film/graphene core–shell	LiF'/AL	Core shell	2.27%
TiO_2 coated CNT fiber	CNT fiber	Intertwined	2.94%
CdSe nanowires grown on Ti wires	CNT yarns	Intertwined	1–2.9%
TiN nanowire	Cu coated polymer wire	Wrapped typed	0.9%
Glass/FTO/ZnO-NP	PEDOT: PSS/AgNW	Stacked	1%
Glass fiber/polyamide/silver/TiO_2 compact layer	PEDOT: PSS/AgNW	Stacked	0.4%
TiO_2 photoanode coated SUS metal ribbon	Pt nanoparticle-loaded carbon yarn	weaved	2.63%
TiO_2 coated glass fiber/ Metal wire (Photoanode textile)	Pt deposited fiber/ Metal wire (Counter electrode textile)	Sewed	5.83%
TiO_2 nanotube array/Ti wire	Carbon nanotube sheet	wrapped	≤5%
TiO_2 nanotube/Ti wire	Carbon nanotube mesh	Wrapped	1.6%
TiO_2 layer /Ti wire	Pt wire	Fiber shaped	6%
Aligned titanium dioxide nanotubes/Ti wire	Aligned CNT fiber	Twisted	4.6%
TiO_2 tube array/Ti wire	CNT film	Twisted/fiber shaped	1.6%
TiO_2 coated carbon fiber	Carbon ink/carbon fiber	Fiber shaped	1.9%
P25@CFE	Gr@CCE	**Stacked Type**	**6%**

2.6 . Perovskite Solar Cells (PSCs)

The practical and effective use of organic–inorganic metal halide perovskites in solar cells used for the development of DSSCs due to the low stability of perovskites in the electrolyte. By using perovskites as photosensitizers in the solid-state DSSCs, it increases the power conversion efficiency (PCE) . Using PSCs with solid state DSSCs increases the efficiency 10% compared to with out Perovskite material PCE 5–7% . The PSCs also used as charge carriers.

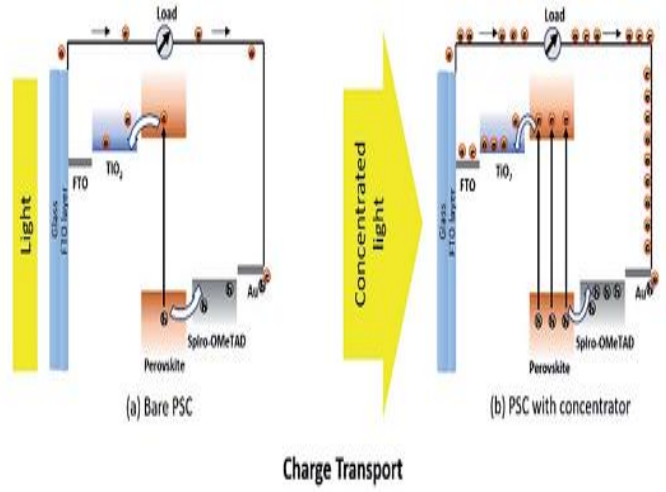

Fig 2.6 Operating principle of perovskite solar cells: charge transport of (a) a bare perovskite solar cell (PSC) and (b) a PSC with a concentrator. **[Reference 10]**

In order to have high PCE , the loss internal energy of the material must be decreased inside the cells . The performance of PSCs can be improved by adding fullerene and its derivatives on the TiO2 surfaces . So it decreases the hysteresis of the I–V curve and increasing the FF to enhance the PCEs. To create excellent electron-transporting layers (ETL) , there should be Phosphonic acid–containing self-assembled fullerene layers on indium–tin oxide (ITO) and the cell employing poly[5,5′-bis(2-butyloctyl)-(2,2′-bithiophene)-4,4′-dicarboxylate-alt-5,5′-2,2′-bithiophene](PDCBT) with Ta–WOx as the hole-transport material (HTM) showed a PCE of over 21% and stability to light stress. In this experimental report amino-alkyl acids were also used as interfacial molecules between TiO2 and the perovskite layer.

In recent research reports summarizes the carbon counter electrodes based PSCs results in different PCE as shown in the table below . In the research process developing Carbon Counter Electrode Materials (CCE) by modification techniques to improve the perovskite/CCE interfacial .The technique is controlling the particle size and thickness of the carbon material to optimize the perovskite/CCE interface and to improve the crystallinity of the perovskite .With this technical configuration results the optimal thickness of the low-temperature processed CCE was 20 μm in the m-TiO2-based PSC . Also it should be take account the stability of the CCE-based device with that of the regular PSC with commonly used metal electrodes (Au and Ag) under the same conditions so that the CCE-based PSC exhibited a better stability than that of the devices using the other CEs because carbon presents a better hydrophobicity than Au and Ag. Here is Key related information of the carbon counter electrodes based PSCs shown below. [Reference 11]

PSC configuration	CCE fabrication technique and sinter	CCE modification technique temperature [°C]	PCE [%]
FTO/c-TiO_2/m-TiO_2/ZrO_2/Cb/spheroidal graphite/$CH_3NH_3PbI_3$	Screen printing, 400	/	6.64
FTO/c-TiO_2/m-TiO_2/$CH_3NH_3PbI_3$/commercial carbon paste	Doctor blading, 100	Low temperature	8.31
FTO/c-TiO_2/m-TiO_2/$CH_3NH_3PbI_3$/carbon ink	Doctor blading, 70	Thickness control	9.08
FTO/c-TiO_2/m-TiO_2(anatase nanosheet)/ZrO_2/Cb/spheroidal graphite/ $CH_3NH_3PbI_3$	Screen printing, 400	/	10.64
FTO/c-TiO_2/m-TiO_2/ZrO_2 /Cb/5-AVA)$_x$(MA)$_{1-x}$ PbI_3	Screen printing, 400	/	12.84
FTO/c-TiO_2/m-TiO_2/ZrO_2 /Cb/5-AVA)$_x$(MA)$_{1-x}$ PbI_3	Screen printing, 400	Oxygen management strategy	15.7
FTO/c-TiO_2/m-TiO_2/ZrO_2/carbon/$CH_3NH_3PbI_3$	Screen-printing, 400	Thickness and particle size control	11.63
FTO/c-TiO_2/m-TiO_2/carbon/CH_3NH_3Pb/FTO	Rolling transfer	Press transfer	11.02
FTO/c-TiO_2/m-TiO_2/$CH_3NH_3PbI_3$/carbon ink	Screen-printing and transfer, 85	Hot press	13.53
FTO/c-TiO_2/m-TiO_2/ZrO_2/ordered mesoporous carbon/$CH_3NH_3PbI_3$	Screen-printing	Formation of porous structure	7.02
FTO/c-TiO_2/m-TiO_2/$CH_3NH_3PbI_3$/carbon	Screen-printing, rm	Formation of mesoporous structure	10.2
FTO/c-TiO_2/m-TiO_2/$CH_3NH_3PbI_3$/carbon	Doctor blading, 70	Encapsulation	10.8
FTO/c-TiO_2/m-TiO_2/ZrO_2/HTC/((5-AVA)$_x$ (MA)$_{1-x}$$PbI_3$)/LTC	Screen-printing, 50	Chemical binder	14.04
FTO/c-TiO_2/m-TiO_2/$CH_3NH_3PbI_3$/carbon	Doctor blading, 100	Solvent effect	13.5
FTO/c-TiO_2/m-TiO_2/$CH_3NH_3PbI_3$/carbon	Doctor blading, 100	Solvent effect	8.32
FTO/c-TiO_2/m-TiO_2/perovskite/HTL/carbon	Transfer and press	Solvent exchange	19.2
FTO/c-TiO_2/m-TiO_2/$Cs_{0.06}(MA_{0.17}FA_{0.83})_{0.95}$ $Pb(I_{0.84}Br_{0.16})_3$/carbon	Screen printing, 100	Solvent dripping	13.57
FTO/c-TiO_2/m-TiO_2/$Cs_{0.05}(MA_{0.17}FA_{0.83})_{0.95}$ Pb $(I_{0.83}Br_{0.17})_3$/SWCNTs/ Spiro-OMeTAD	Press transfer	New materials	16.0
ITO/SnO_2/FACsPbI$_3$/CNTs/Spiro-OMeTAD	Laminating	Doping	17.56
FTO/c-TiO_2/m-TiO_2/$FA_{0.8}Cs_{0.2}PbI_{2.64}Br_{0.36}$/PEO/carbon	Doctor blading, 100	Modification of work function	14.9
FTO/c-TiO_2/m-TiO_2/ZrO_2/$CH_3NH_3PbI_3$/NiO/carbon/	Screen-printing, 50	Modification of work function	14.14
FTO/c-TiO_2/$MaPbI_2Cl$/NiO@carbon sphere	Doctor blading, 50	Composite CCE	11.80
FTO/c-TiO_2/$CH_3NH_3PbI_3$/MAI@carbon	Doctor blading, 50	Composite CCE	13.6
PER/graphene/TiO_2/PCBM/$CH_3NH_3PbI_3$/CSCNTs@Spiro-OMeTAD	Transfer	Composite CCE	11.9
FTO/c-TiO_2/m-TiO_2/ZrO_2/AV-C/$CH_3NH_3PbI_3$	Screen printing, 400	New material	12.58
FTO/c-TiO_2/m-TiO_2/ZrO_2/(5-AVA)$_x$(MA)$_{1-x}$ PbI_3)/ultrathin graphite	Screen printing, 50	New material	14.07
FTO/c-ZnO/$CH_3NH_3PbI_3$/carbon	Doctor blading, rm	Low temperature	8%
FTO/c-TiO_2/$CH_3NH_3PbI_3$/coal based CCE/Al	Spray coating and doctor blading, 90	New material	10.87
ITO/SnO_2/$CsPbIBr_2$/carbon	Doctor blading, 100	SnO_2 passivation	7.0
FTO/TiO_2/SnO_2/$CsPbBr_3$/carbon	Doctor blading, 85	SnO_2 passivation	8.79
ITO/PEN/m-SnO_2/$Cs_{0.05}(MA_{0.17}FA_{0.83})_{0.95}Pb(I_{0.83}Br_{0.17})_3$/PEDOT:PSS/carbon	Screen printing, 70	Friendly conditions	7.04
FTO/c-TiO_2/m-TiO_2/$Cs_x(MA_{0.7}FA_{0.3})_{1-x}PbI_3$/carbon	Doctor blading, 100	Friendly conditions	15.03
FTO/c-TiO_2/m-TiO_2/ZrO_2/$(FA)_{0.3}(MA)_{0.7}PbI_3$ /ordered mesoporous carbon	Doctor blading, 100	Friendly conditions	9.53

3. SUPERCAPACITORS

Supercapacitors are a type of new energy storage devices and their conversion equipment is supposed to have the potential of high power density, great circulation feature, rapid discharge-charge, poor self-discharging, safe working, and low cost. Energy storage supercapacitors are categorized into three types including pseudocapacitive (faradaic supercapacitors) , electrical double layer capacitor or EDLC and hybrid supercapacitors which is most advanced supercapacitor combines the EDLC and pseudo-supercapacitors. The electrical double layer capacitor (EDLC) is the most common type of supercapacitors .The attributes of EDLC is controllable by the connection area between the electrolyte and electrode materials. The better attributes can be achieved by using larger areas and pseudocapacitive supercapacitor can save charge by an electro activation procedure. Supercapacitors represent the alternative to common electrochemical batteries, mainly to widely spread lithium-ion batteries.

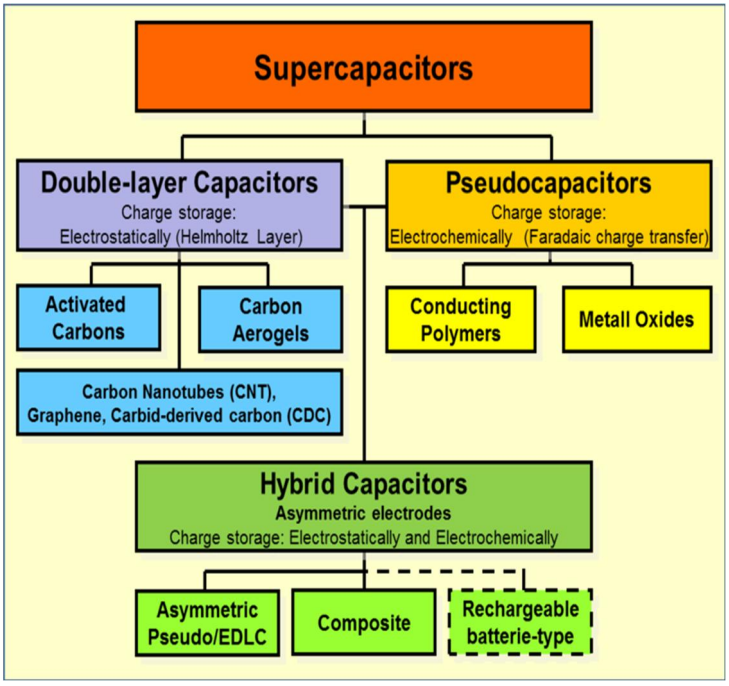

Fig.3.a [Reference : wikiwand]or available in this link : '' https://www.wikiwand.com/en/Supercapacitor''

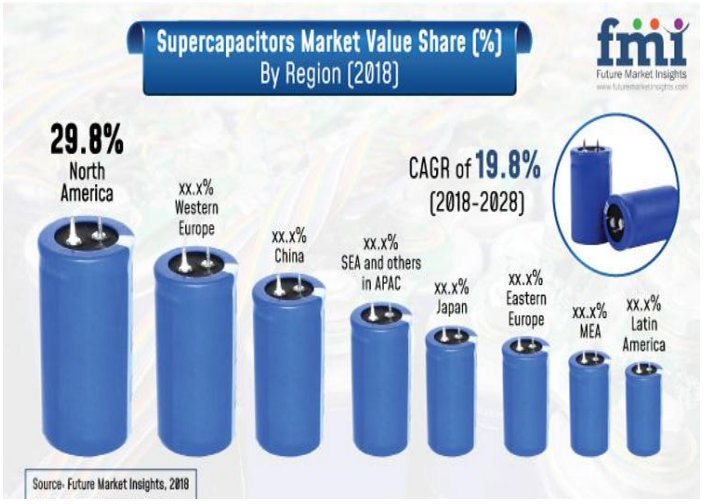

Fig.3 .b

Fig.3. a shows Family tree of supercapacitor types. Double-layer capacitors and pseudo capacitors as well as hybrid capacitors are defined over their electrode designs.

Fig, 3 b. shows Innovations in Supercapacitor Development :-Past, Present, and future also Market Value Share by Region or for other types of super capacitor can be found in the following video link

https://youtu.be/7oGvGR2FxUY

3.1 The basic concepts of EDLC and Faradaic supercapacitors

Electric double layer capacitor (EDLC) is the electric energy storage system based on charge–discharge process (electrosorption) in an electric double layer on porous electrodes, which are used as memory back-up devices because of their high cycle efficiencies and their long life-cycles. The electric double layer capacitor is commonly known and available in commercial market in which uses liquid electrolyte. Most of the electrolytes are aprotic solvents like propylene carbonate (PC), diethyl carbonate (DEC), dimethyl carbonate (DME) or ethylene carbonate (EC), which include dissolved salts like tetraethylammonium tetrafluoroborate ($TEABF_4$) or lithium hexafluoroarsenate ($LiAsF_6$) . The EDLC has Helmholtz double layers on the phase interface

between the surface of the electrodes and the electrolyte for electrostatic interaction to accumulate energy . In EDLC there is no electron exchange and no redox reaction and the energy is stored non-faradaically . The main point for the use of EDLC is to obtain an extremely high capacity which is the large surface of the electrodes and the Helmholtz layer thickness. Generally EDLC supercapacitors have good durability and cycle ability in millions of cycles. Commonly activated carbon (AC) is used as an electrode material for EDLC supercapacitors due to large specific surface area as advantageous. So in electrical double layer capacitor , electrostatic energy storage by separating charges at the interface between the surface of a conductive electrode and an electrolyte without faradaic reactions.

The double-layer serves approximately as the dielectric layer in a conventional capacitor, albeit with the thickness of a single molecule. Thus, the standard formula for conventional plate capacitors can be used to calculate their capacitance.

$$C = \varepsilon \frac{A}{d}.$$

Capacitance C is greatest in capacitors made from materials with a high permittivity ε, large electrode plate surface areas A and small distance between plates d.

Here is the styles of super capacitors.

[Reference : wikiwand]or available in this link : ‘’ https://www.wikiwand.com/en/Supercapacitor’’

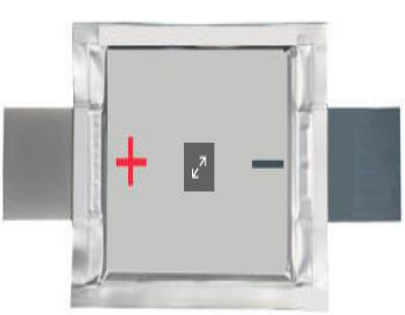

Flat style of a supercapacitor used for mobile components

Radial style of a supercapacitor for PCB mounting used for industrial applications

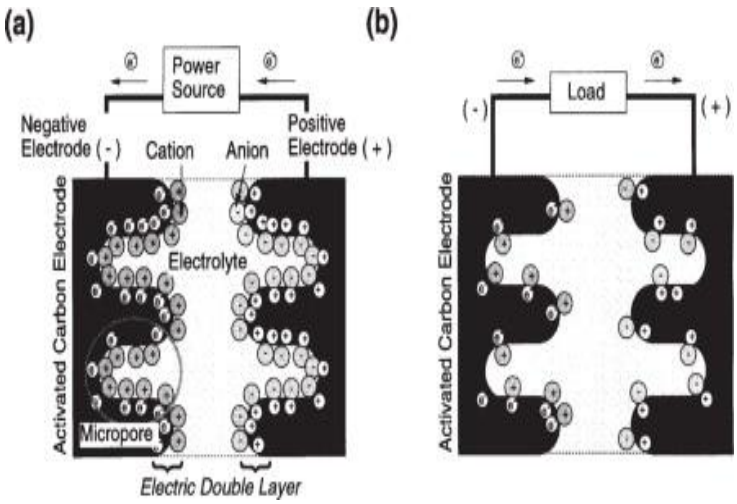

Fig. 3.1a . shows a model of Helmholtz double layer
Fig. 3.1b. Schematic illustration of electric double layer capacitor: (a) charge state, (b) discharge state.

[Reference : wikiwand]or available in this link : ‘’
https://www.wikiwand.com/en/Supercapacitor’’

The second type of supercapacitor is Faradaic supercapacitor or Pseudo capacitance which is the electrochemical storage of electricity in an electrochemical capacitor .This faradaic charge transfer originates by a very fast sequence of
reversible faradaic redox, electrosorption or intercalation processes on the surface of suitable electrodes. Pseudo capacitance is accompanied by an electron charge-transfer between electrolyte and electrode coming from a de-solvated and adsorbed ion. One electron per charge unit is involved. Faradaic pseudo capacitance only occurs together with static double-layer capacitance. Pseudo capacitance and double-layer capacitance both contribute inseparably to the total capacitance value. The amount of pseudo capacitance

depends on the surface area, material and structure of the electrodes. Pseudo capacitance may contribute more capacitance than double-layer capacitance for the same surface area by 100x . Generally faradaic electrochemical energy storage by fast reversible surface redox reactions, intercalation or electro sorption at or near the surface of some electrode materials.

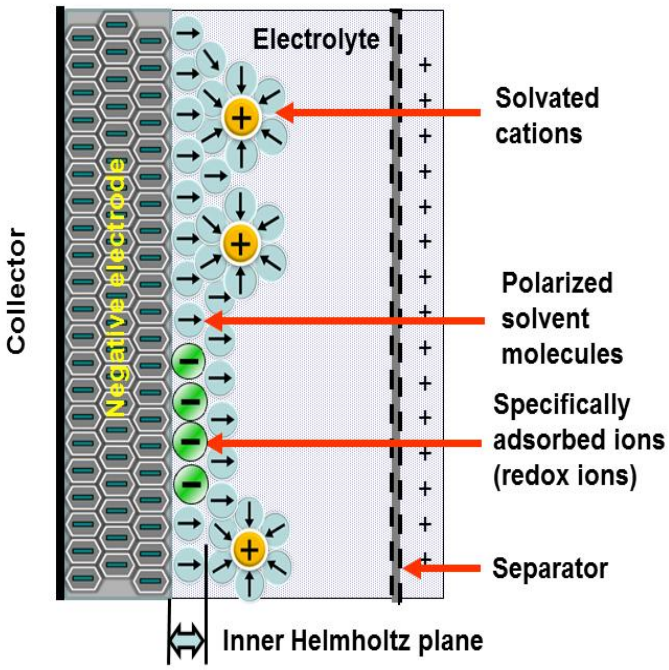

Fig . 3.1c . shows Simplified view of a double-layer with specifically adsorbed ions which have submitted their charge to the electrode to explain the faradaic charge-transfer of the pseudo capacitance. [Reference : wikiwand]or available in this link : '' https://www.wikiwand.com/en/Supercapacitor''

3.2 The different elements of a supercapacitor

For production of supercapacitors , there are different materials used depending on the type of energy storage required by the application at hand and the required capacitance ranges. So presently significant number of materials are available for the construction of supercapacitors . The most commonly used material is carbon , which is widely used and can be converted into many forms. The other materials include Current collectors (metals, wires, carbon based), active materials (carbon based + metal-oxides + binders), separators (polymers or ceramics…) and liquid electrolytes (aqueous based, organic solvent based, ionic liquids) .

Electric double layer capacitors	▪ Carbon aerogels ▪ Activated carbons ▪ Carbon fibers ▪ Carbon nanotubes
Pseudo-capacitors	▪ Metal oxides ▪ Conducting polymers
Hybrid capacitors ❑ **Asymmetric** ❑ **Composite** ❑ **Battery-type**	▪ Carbon materials, conducting polymers ▪ Carbon materials, metal oxides

The above table shows Classification of supercapacitor types and their electrode materials.

Carbon Materials

Activated carbons find application in electrodes for EDLC supercapacitors, in which they are commonly used materials. These carbons are important for their large surface area due to their highly porous structure and less expensive than other carbon materials. More recently, supercapacitors are increasingly based on carbon nanotubes (CNTs). CNTs have unique material properties that make them highly applicable as a supercapacitor material. The most important features of CNTs are their electronic, mechanical, optical, and chemical characteristics. They exhibit excellent electronic conductivity and some highly desirable mechanical properties. Supercapacitor electrodes made from CNTs have a continuous charge distribution utilizing most of the surface area that helps the CNT based electrodes to achieve capacitances comparable to those in activated carbon electrodes, despite the larger surface area in activated carbon. The other type of carbon is carbon aerogels are typically used in EDLC supercapacitors made of continuous networks of carbon nanoparticles with

interspaced mesopores, which allows them to be used in electrodes without the need for a binder material . This materials exhibit lower equivalent series resistance, which helps in increasing power performance.

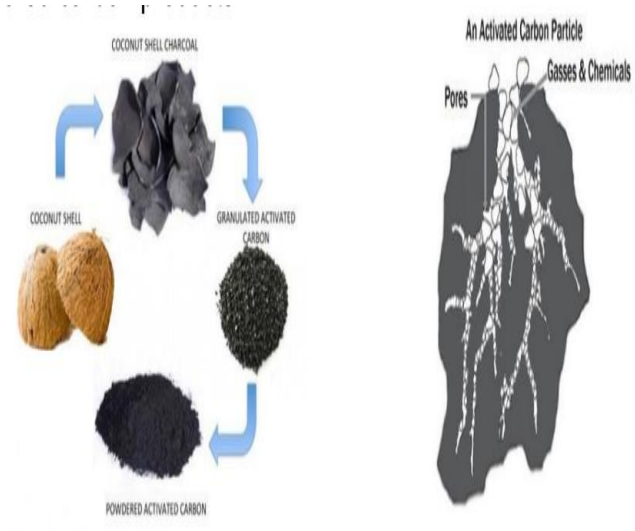

Fig 3.2 shows Carbon based nanomaterials .[Reference :- The picture is taken from supercapacitor pdf slides from Nanomaterials and nanotechnologies for energy application course]

Active materials

The most widely used active materials are carbon based + metal-oxides + binders. Activated carbon was the first material chosen for EDLC electrodes. Even though its electrical conductivity is approximately 0.003% that of metals which is sufficient for supercapacitors. Activated carbon is an extremely porous form of carbon with a high specific surface area and Solid activated carbon also termed consolidated amorphous carbon (CAC) is the most used electrode material for supercapacitors . It may be cheaper than other carbon derivatives and produced from activated carbon powder pressed into the desired shape, forming a block with a wide distribution of pore sizes. An electrode with a surface area of about 1000 m^2/g results in a typical double-layer capacitance of about 10 $\mu F/cm^2$ and a specific capacitance of 100 F/g. The other information that as of 2010 virtually all commercial supercapacitors use powdered activated carbon made from coconut shells in which Coconut shells produce activated carbon with more micropores than does charcoal made from wood.

Liquid electrolytes

Electrolytes consist of a solvent and dissolved chemicals that dissociate into positive cations and negative anions, making the electrolyte electrically

conductive. The more ions the electrolyte contains, the better its conductivity. In supercapacitors electrolytes are the electrically conductive connection between the two electrodes . They are the main actors in the charge storage mechanism of an electrochemical cell. The electrolyte must be chemically inert and not chemically attack the other materials in the capacitor to ensure long time stable behaviour of the capacitor's electrical parameters. The electrolyte's viscosity must be low enough to wet the porous, sponge-like structure of the electrodes. They can be aqueous, organic or molten salts (ionic liquids).

Water is a relatively good solvent for inorganic chemicals. Treated with acids such as sulfuric acid (H_2SO_4), alkalis such as potassium hydroxide (KOH), or salts such as quaternary phosphonium salts, sodium perchlorate ($NaClO_4$), lithium perchlorate ($LiClO_4$) or lithium hexafluoride arsenate ($LiAsF_6$), water offers relatively high conductivity values of about 100 to 1000 mS/cm. Aqueous electrolytes have a dissociation voltage of 1.15 V per electrode (2.3 V capacitor voltage) and a relatively low operating temperature range. They are used in supercapacitors with low specific energy and high specific power.

Electrolytes with organic solvents such as acetonitrile, propylene carbonate, tetrahydrofuran, diethyl carbonate, γ-butyrolactone and solutions with quaternary ammonium salts or alkyl ammonium salts such as tetraethylammonium tetrafluoroborate ($N(Et)_4BF_4$]) or triethyl (metyl) tetrafluoroborate ($NMe(Et)_3BF_4$) are more expensive than aqueous electrolytes, but they have a higher dissociation voltage of typically 1.35 V per electrode (2.7 V capacitor voltage) and a higher temperature range. The lower electrical conductivity of organic solvents (10 to 60 mS/cm) leads to a lower specific power .

Ionic electrolytes consists of liquid salts that can be stable in a wider electrochemical window, enabling capacitor voltages above 3.5 V. Ionic electrolytes typically have an ionic conductivity of a few mS/cm, lower than aqueous or organic electrolytes.

Separators

Separators physically separate the two electrodes to prevent a short circuit by direct contact. It can be very thin (a few hundredths of a millimeter) and must be very porous to the conducting ions to minimize the equivalent series resistance(ESR). Furthermore, separators must be chemically inert to protect

the electrolyte's stability and conductivity. Inexpensive components use open capacitor papers. More sophisticated designs use nonwoven porous polymeric films like polyacrylonitrile or Kapton, woven glass fibers or porous woven ceramic fibres.

Collectors

The current collector is generally obtained with conductive materials and it mainly acts as contact to access the active material and its stored charge. Current collectors connect the electrodes to the capacitor's terminals. The collector is either sprayed onto the electrode or is a metal foil. They must be able to distribute peak currents of up to 100 A.

3.3 The principal characterization methods (I -V curves, Quantum efficiency, EIS, …)

I -V curves

To see the I-v curves of supercapacitors a galvanostatic charge/discharge device is used with curves of the supercapacitors assembled with PVA-KOH and poly(vinyl alcohol) (PVA)- potassium hydroxide (KOH)-hydroquinone (HQ) (PVA-KOH-HQ) based gel polymer electrolyte (GPE) at a current density of 0.8 A g^{-1} . The specific capacitance(Cs) of the electrodes for both electro chemical materials are 107.06 and 326.53 F g^{-1} , respectively, at a charge/discharge current density of 0.8 A g^{-1} . This shows the specific capacitance(Cs) of the supercapacitor with PVA-KOH-HQ based GPE is larger than that of the one with PVA-KOH based GPE and the capacitive property of the supercapacitor improved by the redox mediator HQ. When the supercapacitor is in charging condition , hydroquinone is oxidized into quinone with $2H^+$ and 2 electrons, and during the discharge process, quinone is reduced into hydroquinone via the gain of 2 electrons with $2H^+$ at the corresponding oxidation and reduction potentials. The hydroquinone shows pseudo capacitance at the electrolyte-electrode interface and significantly contributes to the total electrode-specific capacitance of the supercapacitor.

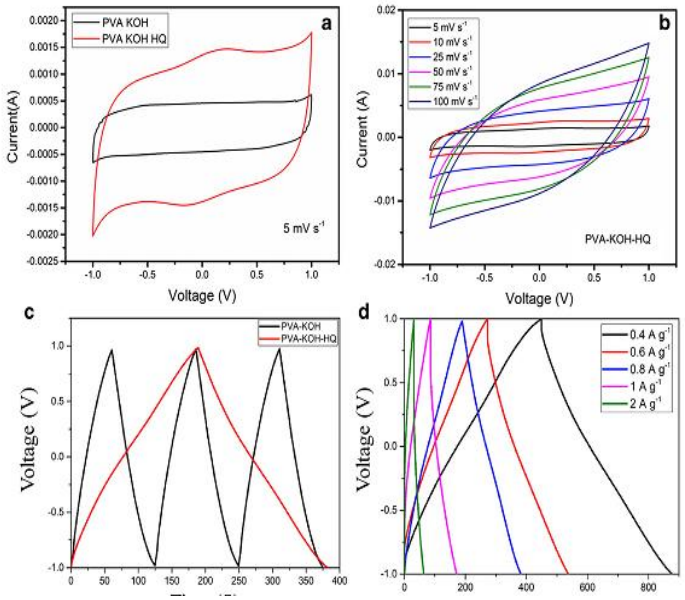

Fig. 3.3a. a. CV curves of the supercapacitors with PVA-KOH and PVAKOH-0.2 g HQ based GPEs at a scan rate of 5 mV s−1 . b. CV curves of the supercapacitor with PVA-KOH-0.2 g HQ based GPE at scan rates of 5 to 100 mV s−1 . c. galvanostatic charge discharge (GCD) curves of the supercapacitors with PVA-KOH and PVA-KOH-0.2 g HQ based GPEs at 0.8 A g−1 current density. d . GCD curves of the supercapacitor with PVA-KOH-0.2 g HQ based GPE at current densities from 0.4 to 2 A g−1. [Reference 12]

Electrochemical Impedance Spectroscopy Model for a Super-capacitor

Electrochemical Impedance Spectroscopy (EIS) is one way of measuring the equivalent series resistance (ESR) of super-capacitors and it can measure capacitance and capacitor non-ideality. For modelling supercapacitor , a simplified Randles model is used .

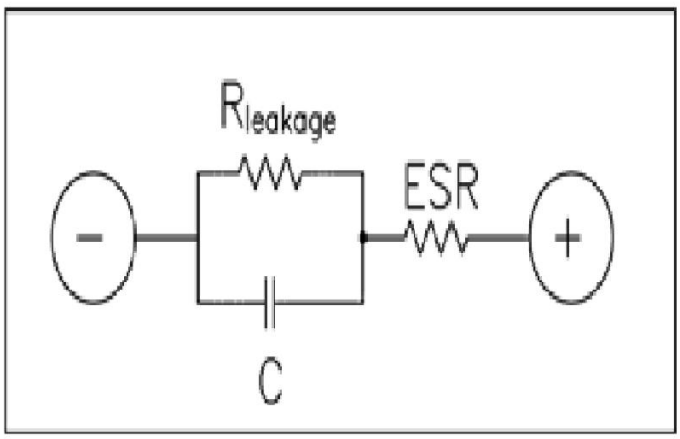

Fig. 3.3b . shows that Randles equivalent circuit for modelling super-capacitors.

[Reference :- available in the following link ‘‘ https://www.gamry.com/application-notes/battery-research/testing-electrochemical-capacitors-cyclic-voltammetry-leakage-current/’’]

By using Gamry’s EIS300 , it can measure EIS using three different control systems . These methods are Potentiostatic EIS ,Galvanostatic EIS and Hybrid EIS .The galvanostatic system control the cell current where as the Potentiostatic system cell voltage .The hybrid system uses the galvanostatic cell control but varies the AC current to maintain a fixed AC-voltage response. On other hand galvanostatic and hybrid system EIS are preferred for very-low-impedance cells and small errors in the DC voltage can create huge DC currents. The impedance of the 3 F capacitors used to generate data and Potentiostatic system is the most common EIS system which is selected in this report.
The EIS Spectra on a 3 F EDLC at Different Potentials

The Gamry Sequence Wizard was also used to record these data. The loop contained both an equilibration step and EIS data-acquisition.

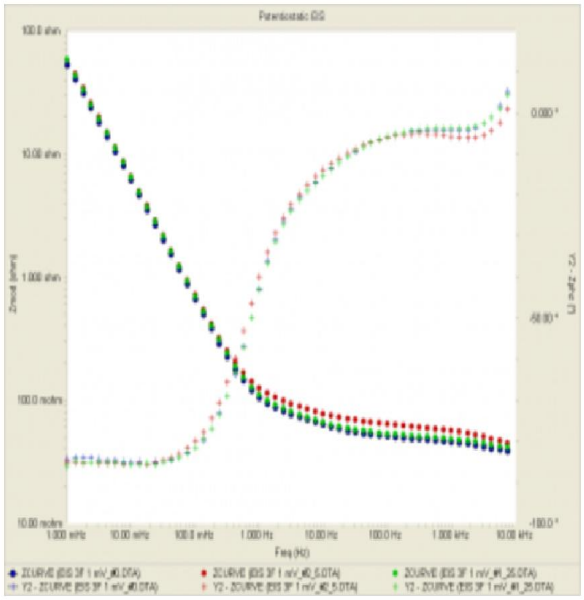

Fig. 3.3c . Shows that Bode plot of 3 F EDLC at 0.0 V (blue), 1.25 V (green), and 2.50 V (red).

[Reference :- available in the following link ‘‘ https://www.gamry.com/application-notes/battery-research/testing-electrochemical-capacitors-cyclic-voltammetry-leakage-current/’’]

From the above figure a Bode plot of EIS spectra of a 3 F EDLC recorded at three DC potentials: 0.0, 1.25 and 2.50 V (in blue, green and red) and the capacitor was held at the DC voltage for 10 min between spectral acquisitions.

3.4 Flexible SC

In recent years the growth of flexible supercapacitors is increasing . For the construction of flexible supercapacitors different materials are used . In this report we see solid-state graphene-based flexible supercapacitor ,with the goal of maintaining their high electrochemical performance while following the significant trend of portable and wearable electronics becoming small, thin, lightweight, and flexible, which brings new challenges for energy-storage systems. It is well known that graphene is the best material component for the fabrication of flexible electrodes because of its exceptionally high mechanical strength, excellent surface area and good conductivity.

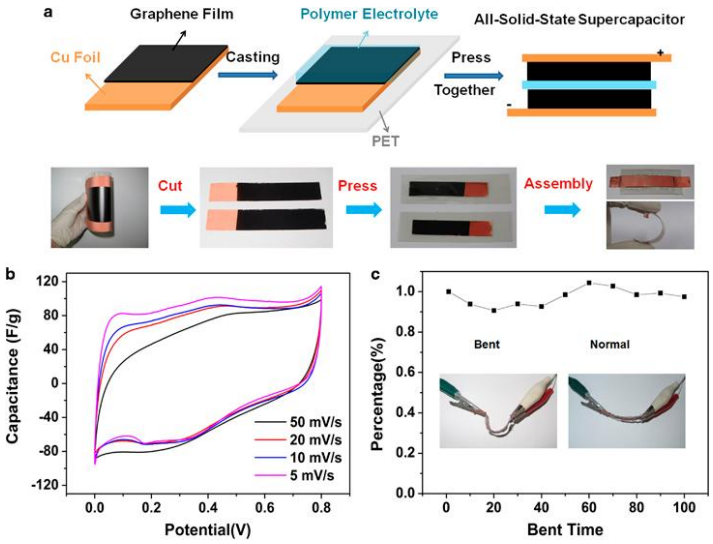

Fig.3.4a. Schematic diagram of fabrication of flexible supercapacitor device [Reference :- the picture available in the following link

‘‘ https://www.researchgate.net/figure/Schematic-diagram-and-photographs-of-the-fabrication-process-of-flexible-all-solid-state_fig1_275203466 ’’

Substrate Materials for Flexible Supercapacitors.

Substrate Materials play a great role in the fabrication of a flexible supercapacitor electrode for mechanical flexibility and strength to the electrode components . So the most commonly materials used in the construction of flexible supercapacitors are nickel foam along with aluminium foam or foil, graphite sheets, and carbon cloths due to their high conductivity, flexibility and high porosity. In recent reports shows that the utilization of carbon nanofibers (CNFs) in the fabrication of supercapacitor electrodes because it provides excellent properties such as a high conductivity, very high specific surface area and mechanical flexibility. Carbon nanofibers (CNFs) synthesized by polymer carbonization process in which many polymers used to form carbon nanofibers. The most common polymers used for the production of carbon nanofibers are poly(acrylonitrile) (PAN) and poly(vinyl alcohol) (PVA) because of their high carbon content upon carbonization. First of all the polymer is dissolved in solvent to form a polymer solution then subjected to an electrospinning process by applying high potential (10−15 kV), then the solution forms continuous fibers with an average diameter of several microns to nanometres . Then polymerized nanofibers are then introduced to a carbonization process.

GRAPHENE NANOCOMPOSITE BASED ON TYPES OF ELECTRODE MATERIALS

1. Additives/Binder Added Electrodes.

   In this Additives/Graphene Electrodes fabrication carbon black (CB) has often been used as a conductive additive due to s high conductivity and low cost and reduced graphene oxide (rGO) was mixed with different amounts of CB and subjected to vacuum filtration to obtain the nanocomposite film . So the rGO/CB film was free-standing and has flexible properties.

   For Binder/Graphene Electrodes fabrication mesoporous graphene was utilized by mixing 10 wt % Polytetrafluoroethylene (PTFE) binder and 5 wt % super-p, which was then made into coin-size capacitor cells and the electrodes were separated via a Celgard porous membrane and 1-ethyl-3-methyldizolium tetrafluoroborate (EMIMBF4) as the organic electrolyte.

2. Binder-Less Electrodes

It has different advantages including a cost reduction (from eliminating the binder cost) and minimization of the electrical interference between the components at the interface. It has the following components :-

a. Pure Graphene Electrode.

It can be produced directly with out any process 2D “in-plane” pristine graphene and reduced multilayer graphene oxide (RMGO) in which the pristine graphene was synthesized via the CVD technique and the multilayer graphene films were synthesized via the chemical reduction of graphene oxide. The electrolyte used for the active surface and the gap between the electrodes is an acidic polymer electrolyte (PVA/H3PO4) . Here the in-plane design involved isolating a large planar sheet of graphene into two electrodes by creating a micro meter-sized gap through the graphene layer and then sputtering the external edges of the two electrodes with gold as current collectors. So this combination results a fabricated device with ultrathin, flexible, and optically transparent features. In this case the G- electrode showed a normalize capacitance of 80 µF cm−2 based on the CV curve but the capacitance of the RMGO device was approximately five times higher (390 µF−2).

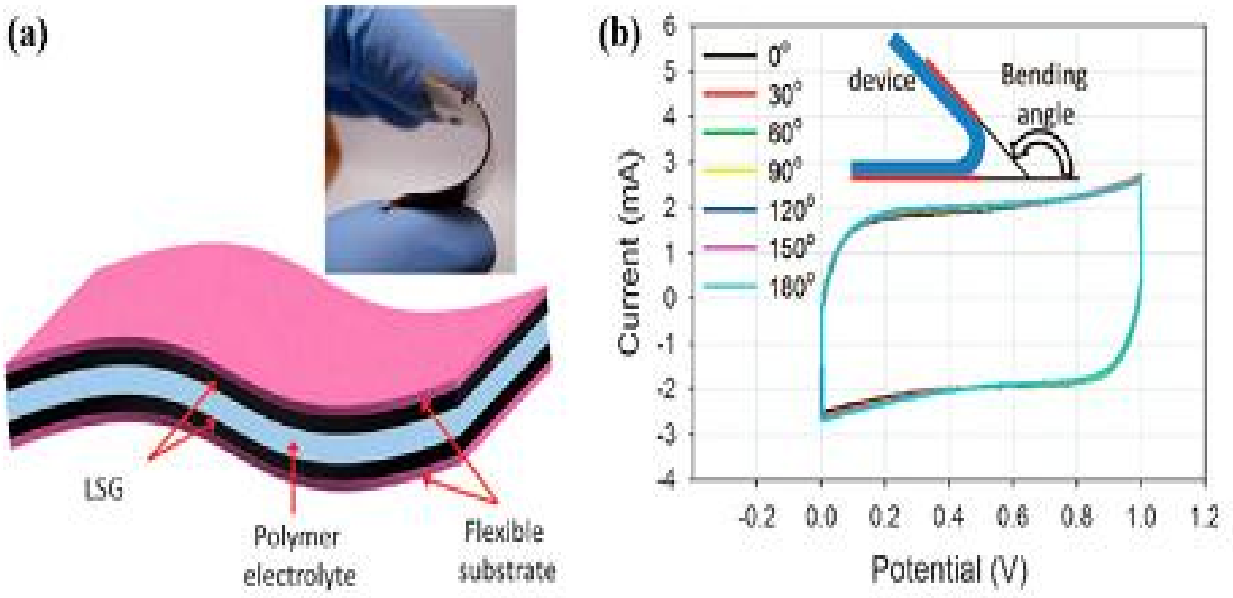

Fig. 3.4b. (a) Design and fabrication of flexible, all-solid-state laser-reduced graphene (LSG) electrochemical capacitor. (b) Bending the device had almost no effect on its performance [Reference 13]

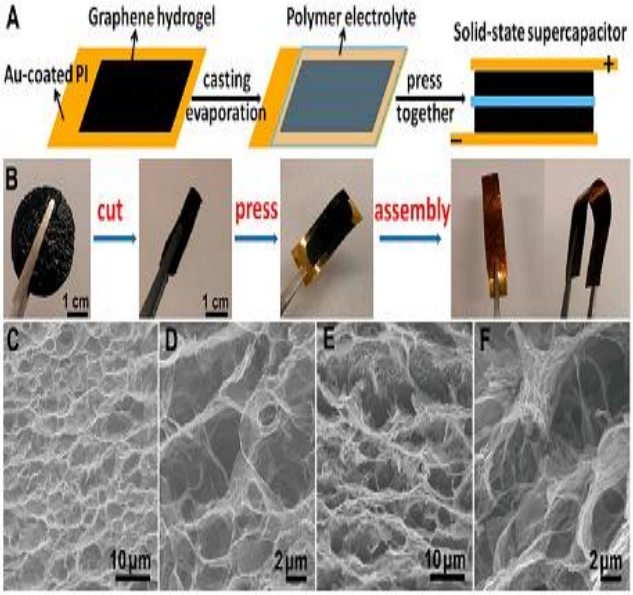

Fig. 3.4c . (a) Schematic diagram and (b) photographs of fabrication process for flexible solid-state supercapacitors based on graphene hydrogel films.(c) Low- and (d) high-magnification SEM images of the interior microstructure of the graphene hydrogel before pressing. (e) Low- and (f) high magnification SEM images of the interior microstructure of the graphene hydro gel film after pressing. [Reference 14]

b. Symmetrical Supercapacitor which has in its components :-

1. Conductive Polymers/Graphene Composites Electrode.

   This graphene/polyaniline (PANI) produced as a stretchable supercapacitor electrode through a continuous chemical growth methods. In the process the nickel foam template was completely removed then rest only porous graphene template behind and the graphene sheet was subsequently pulse electrodeposited with PANI. In this way a stretchable supercapacitor device produced by immersing the identical electrodes in PVA/H3PO4 polymer electrolyte and stacking the electrodes together.

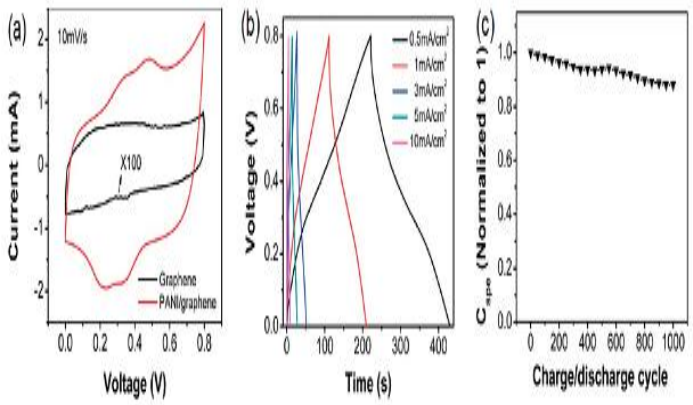

Fig. 3.4d . (a) Porous graphene electrodes with and without PANI at scan rate of 10 mV s−1 . (b) Galvanostatic charge/discharge curves of the stretchable supercapacitor with PANI/graphene electrodes at different current densities. (c) Cycling performance of the stretchable supercapacitor with PANI/ graphene electrodes for charging and discharging at a current density of 1 mA cm−2 . [Reference 15]

2. Metal/Metal Oxides Composite Electrode.

   This method is preparation of MnO2-coated graphene fiber by direct electrochemical deposition of MnO2 onto a graphene fiber network. So by this method a flexible solid-state device was then fabricated by intertwining two MnO2/G/GF electrodes separated by a PVA/H2SO4 polymer gel electrolyte.

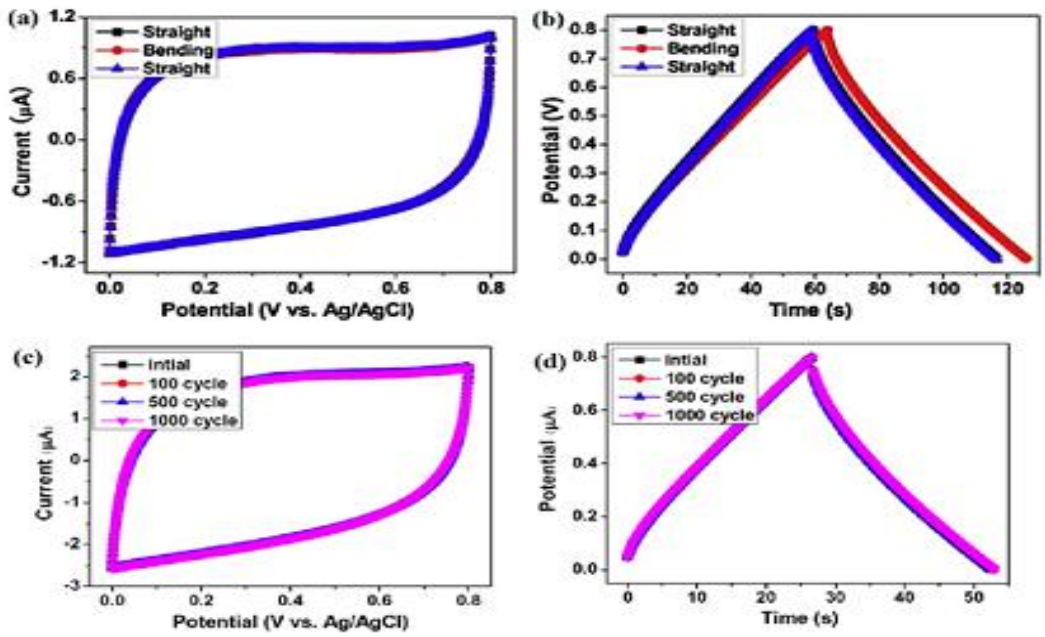

Fig.3.4e . (a) CV at a scan rate of 10 mV s−1 and (b) charge/discharge curves of the fiber capacitor at a current of 1 mA, with an effective length of 0.5 cm under straight and bent conditions. (c) CV at a scan rate of 25 mV s−1 and (d) charge/discharge curves of 1.3 cm long MnO2/G/GF fiber supercapacitor at 2 mA of applied current, with different straight/bending cycles. [Reference 16]

3.5 Wearable SC

Supercapacitors are one of the best energy storage device for wearable electronic devices. They have an anode, cathode, and a separator but energy storage mechanism is different from that of batteries . They store energy on the surface of the electrodes by an electrochemical double layer (EDLC) or pseudocapacitive mechanism and provide high power densities, long cycle life, and rapid charging–discharging rates

3.5.1 Supercapacitor Fibers.

Recently modern energy storage supercapacitors have been fabricated in different configurations for portable and wearable electronic devices. These configurations are flexible yarn supercapacitors , fiber/ cable type Supercapacitors and Screen Printed Supercapacitors which provide flexible, lightweight, shape conformable and mobile usable characteristics for supercapacitors. Lets see one by one.

a. Flexible Yarn Supercapacitors

They have linear or 1D structure having more advantageous than that of 2D and 3D planar structures . They are produced from fiber electrodes have an interlaced structure, which allows the constituent filaments to move freely relative to each other providing freedom for body movements and permeability to air and moisture. Flexible yarn supercapacitors are produced on linear substrates such as metal wires, plastic/rubber wires, carbon wires, carbon nanofibers, CNT yarns, CNT nanocomposites fibers, graphene fibers, and graphene composite fibers. The typical materials used in flexible yarn supercapacitors are carbon nanoparticles, metal oxides and conducting polymers . Many device architectures designed for yarn supercapacitor, such as biscrolled or two-ply yarn, multi-ply yarn, braided, core–shell, and coaxial yarns. For fiber supercapacitors both symmetric and asymmetric configurations developed . Wang et al. developed a two-ply yarn supercapacitor by twisting a continuous CNT web drawn from solid state MWCNT forest and ordered polyaniline(PANI) nanowire of 50 nm in diameter and 400 nm in length (CNT@PANI yarn). For high capacitance electrode material, PANI maximizes the performance of the thread-like supercapacitor. Polyvinyl alcohol (PVA) gel electrolyte was coated on the surface that acts as both a separator and an electrolyte making the CNT@PANI@PVA composite.

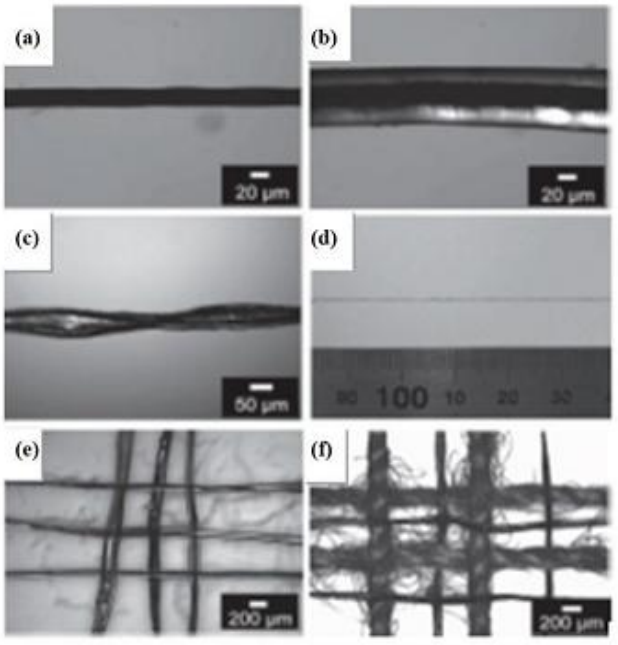

Fig.3.5.1a Optical microphotographs. a) CNT@PANI yarn; b) CNT@PANI@PVA yarn; c) two CNT@PANI@PVA single yarns twisted together to form a thread-like, two-ply yarn supercapacitor. d)

Photograph of a longer supercapacitor. e) A model woven energy storage device consisting of six two-ply yarn supercapacitors (reflection mode). f) Yarn supercapacitors are cowoven with conventional cotton yarns to form a flexible electronic fabric with self-sufficient power source. [Reference 17]

b. Fiber/Cable Type Supercapacitors

They are fabricated by replacing CNT with metal oxide for the development of pseudo capacitors with higher energy density and there is a challenge to make nanostructures of these pseudocapacitive materials in the form of fibers/cables. Recently developed fiber type supercapacitors reported by Wang and co-workers developed a fiber electrode by growing ZnO nanowires on a Kevlar fiber and ZnO nanowires grown on PMMA fiber with the same fiber electrode in which gold deposited on ZnO nanowires for electrical conductivity. The fiber is assembled by twisted together the PMMA fiber around the Kevlar fiber with the electrolyte inside .To improve the specific capacitance ZnO nanowires were electrochemically deposited with MnO2 having specific capacitance of 2.4 mF cm−2 in PVA/H3PO4 gel electrolyte.

The other recently developed cable supercapacitor is integrating energy storage and electrical conduction into a single cable fabricated by an inner electrical cable for electrical transmission and CuO nanowhiskers (CuONW) on the outside of the same cable for energy storage. A copper foil is formed as a tube with CuONW inside as the second electrode then the two electrodes attached together using PVA electrolyte . The region which used as charge storage consists of a high aspect ratio CuO@AuPd@MnO2 (AuPd–gold–palladium) core–shell NWs.

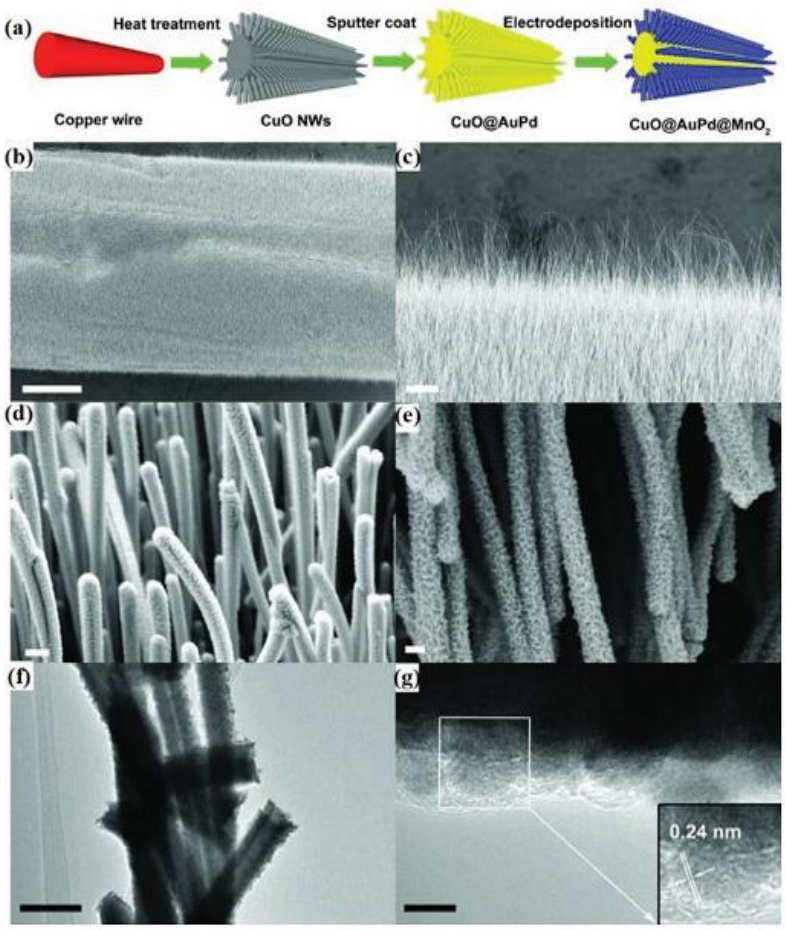

Fig.3.5.1b a) Schematic illustration showing the fabrication process of CuO@AuPd@MnO2NWs. SEM image showing b) CuO NWs completely covering the copper wire. c) Vertically grown CuO NWs. d) AuPd nanoparticles that were conformally sputter-coated onto each NW. e) Uniformly electrodeposited MnO2onto NWs. f) TEM image of CuO@AuPd@MnO2NWs. g) HRTEM image of CuO@AuPd@MnO2NW. [Reference 17]

c. Screen Printed Supercapacitors

The above two fiber supercapacitors are used as wearable energy storage device but screen printed supercapacitors are developed as an energy source due to lightweight, non toxic and non flammable. The recently developed screen printed supercapacitors using porous activated carbon (AC) taken from coconut shells (YP17) was conducted by Jost et al . Inaddition to this various basic and complex arrays of fabric like cotton lawn, polyester microfiber, cotton twill, double knit with silver and nylon neoprene were also studied.

Carbon slurry which is used as screen printing is produced by mixing AC with 5 wt% Liquitex the symmetrically two-electrode device was fabricated using PTFE separator and liquid electrolyte which is surrounded inside a polypropylene bag . In this screen printed supercapacitors the capacitance achieved from the cotton lawn (a hydrophilic natural staple fiber)polyester microfiber (a high wicking fiber with 10 µm diameter) was better than other fabrics . The cotton lawn has a lower mass (6.8 mg cm−2), resistance (3 Ωcm2) and similar capacitance (85 F g−1) when compared to polyester.

On other hand with a similar procedure inactive cotton and polyester backbone replaced with highly conductive knitted and weaved CFs as the backbone of the supercapacitor then AC paint used as the active material and silicotungstic acid solid polymer as the electrolyte. Then CF electrodes woven into green wool with a layer of AC ink screen printed on them as shown in the figure below with dimensions 2 ×3 cm^2 . So this machine used as knitting 3D printer as fast prototyping machines for mass scalability. In this work a solid electrolyte is used for wearable applications with out leaks and they have high average mass loading of 12 mg cm^{-2} than the woven device with 6 mg cm^{-2}. There capacitances are different electrodes with low mass loading provide high capacitance and for high mass less capacitance .

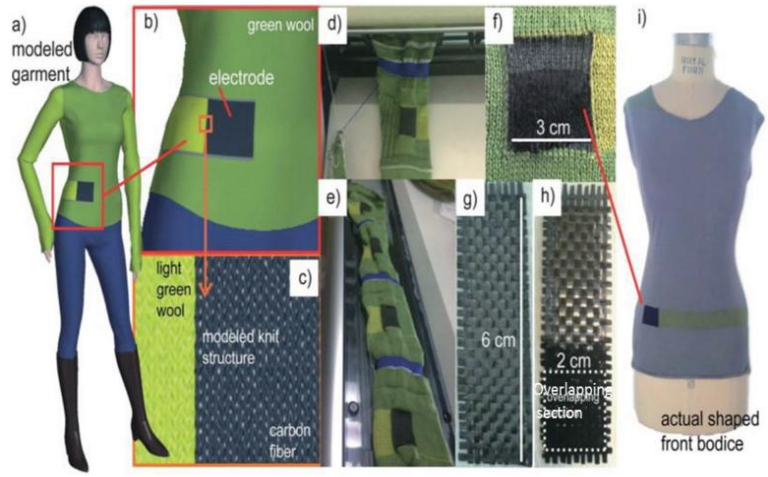

Fig. 3.5.1c . Seamlessly knitted and woven carbon fiber electrodes. a) 3D simulated model. b) Embedded textile supercapacitor in the shirt. c) Simulated nit structure rendered before fabrication. d) Carbon fiber current collector coming out of the knitting machine during fabrication. e) Four current collectors knitted at once. f) CF electrode screen printed with AC. Carbon fiber

woven fabric g) before and h) after printing. i) A shaped front bodice knitted as one piece with a sample electrode made as a part of the textile. [Reference 17]

4. INTEGRATION AND DEVICE FABRICATION

Many solar cells technologies like dye-sensitised, organic, perovskite and silicon integrated with supercapacitors like double layer, pseudo-capacitors and hybrid integrated with many approaches to fabricate solar capacitor devices .To fabricate a fully integrated device both the solar cells and super capacitors must have a common electrode or they must be fabricated from the same substrate . So the electrode facilitates the charge transfer between the solar cells and the supercapacitors by reducing resistance losses in their wires . Most of the structures of integrated photo supercapacitor devices have a planar (monolithic) structure or a fibre-shaped configuration as shown in the fig. below .

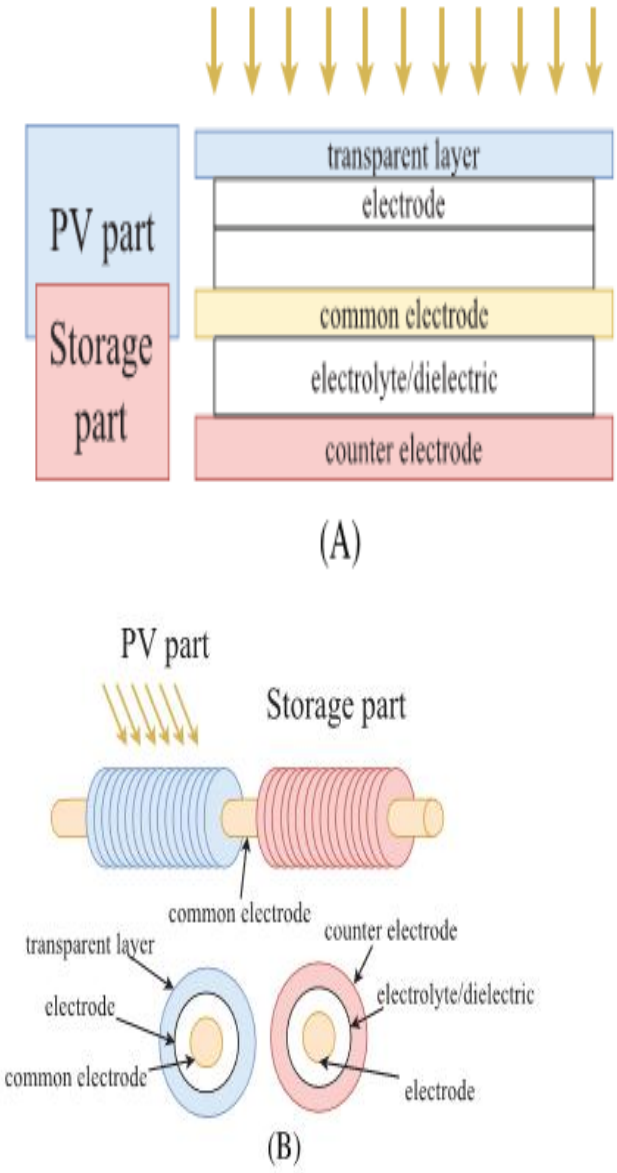

Fig. 4 A, Planar or monolithic three-electrode structure; B, coaxial fibre parallel structure [Reference 18]

4.1 Planar structure

In this case , the solar cell is shown on the top of the device to receiving the incident light and the supercapacitor is shown at the bottom of the device for storage part .They are connected in series . There are three ways of material configuration :- two-electrode, three-electrode, and four-electrode modes.

The two electrode mode is commonly used approach for photo supercapacitor device fabrication except for DSSC due to two problems. The one problem is during discharging , the electron are not able to pass through the TiO2 layer towards the shared electrode and the second one is diffusion of iodine ions causes the SC electrolyte short circuited or self-discharged the device . So these problems results in lower efficiency in comparison with a three-electrode mode.

For DSSC configuration with supercapacitor , an intermediate electrode or the 3rd electrode is added to separate the DSSC and the SC . It has a double function, for a redox electron transfer surface and as charge storage.

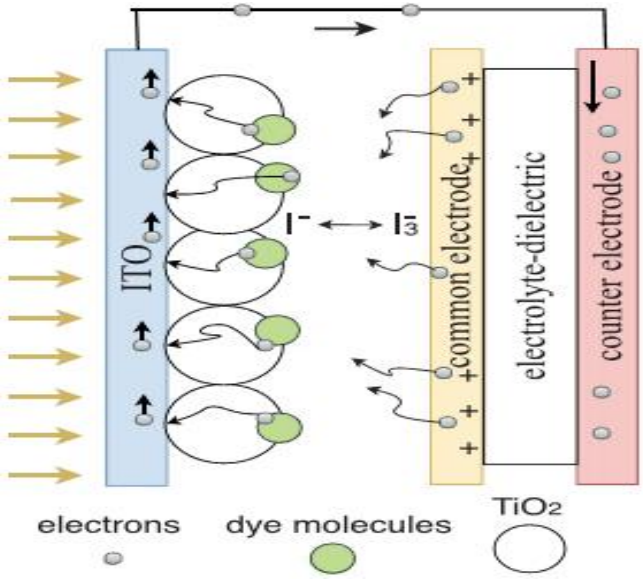

Fig. 4.1 Working principle of a dye-sensitised solar cell coupled with a supercapacitor [Reference 18]

4.2. Fibre structure

The principle of constructing fibre shape device is the same as that of the planner one but the difference is the arrangement of the components looks like core-shell (or coaxial), twisted and parallel-like structures . These devices have common substrate in the form of a fibre. Plastic, elastic rubber, and metal wires have been used as

mechanical support and to assemble the solar cell part and the SC in cores-shell structures .

4.3 . organic solar cells (OSC) or perovskite solar cells (PVSC) integration

organic solar cells integrated with supercapacitors for many applications in the form of portable and wearable device configuration . They have flexibility, lightweight, low costs ,ease of manufacturing (roll-to-roll) underline and transparency criteria's. For the construction of more efficient and powerful integrated devices , perovskite solar cells (PVSC) and SC integration gives the best result . Reports showed that the combination of PVSC and SC results in the device with the highest PV output (13.6 mW cm^{-2}) ,capacitance per unit area (572 mF cm^{-2}) and the efficiency is above 10%.

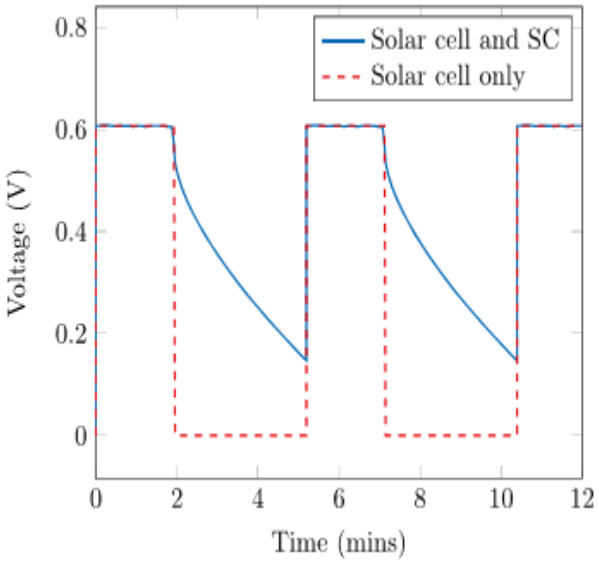

Fig. 4.3 Response of a single solar cell and a solar cell coupled with a supercapacitor during intermittent illumination. If light is on, the voltage of a single solar cell is around 0.6, but when light is off, the voltage decreases to 0. In cases where an appropriate SC is used, the system voltage does not decrease to zero intermediately in the absence of light. This figure is based on Ouyang et al,16 where the illumination period was 2 min followed by a 3-min discharging process at a constant discharging current density of 40 µA cm^{-2}. [Reference 18]

The overall efficiency (ηss) of an integrated device is given by :-

$$\eta ss = \eta sc * \eta s$$

where ηsc is solar cell efficiency and ηs energy storage efficiency.

Here in the table below summarizes comparison of reported integrated devices based on SC and solar cells for energy conversion and storage. [Reference 19]

Devices	PCE	Power density	Energy density	Capacitance	Columbic efficiency	Overall efficiency
DSSC part	4.56%	—	—	—	—	—
SC part	—	4.2 mW cm^{-2}	0.95 μW h cm^{-3}	19 mF cm^{-2}	—	—
SC&DSSC	—	—	—	—	—	2.1%
PSC part	9.00%	—	—	—	—	—
SC part	—	—	—	155 F g^{-1}	—	—
SC&DSSC	—	—	—	—	—	5.07%
PSC part	1.01%	...	...	...	...	...
SC part	...	...	...	0.077 mF cm^{-1}	...	...
SC&DSSC	...	...	...	...	...	0.82%
PSC part	6.2%	...	...	...	...	...
SC part	...	...	...	130 mF cm^{-2}	...	...
SC&PSC	...	...	...	...	...	1.57%
PeSC part	13.6%	...	...	...	...	...
SC part	...	...	...	572 mF cm^{-2}	...	...
SC&PeSC		...	...	...	...	10%
PeSC part	0.46%	...	...	...	...	...
SC part	...	...	...	150 mF cm^{-2}	...	...
SC&PeSC	...	...	...	30 mF cm^{-2}	...	...
PeSC part	6.37%	...	...	...	...	...
SC part	...	7.4 mW cm^{-2}	0.783 μW h cm^{-3}	...	...	...
SC&PeSC	...	...	...	...	...	4.70%
PeSC part	16.1%	...	...	...	...	...
SC part	...	...	...	150 F g^{-1}	...	...
SC&PeSC	...	...	...	...	...	10.97%
Si solar cell	14.9%	...	...	...	...	...
SC part	...	4.6 W cm^{-2}	5 μW h cm^{-3}	...	...	...
SC&Si solar cells	...	...	...	...	62%	...
Si solar cell	14.8%	...	...	...	...	...
SC&Si solar cells	...	...	...	0.14 F m^{-2}	84%	...
hybrid cell	13.39%	...	...	...	...	...
SC par	...	...	...	234 mF cm^{-2}	...	...
SC&hybrid cell	...	...	...	...	...	10.5%
hybrid cell	12.37%	...	...	...	...	...
SC part	...	...	...	16.37 mF cm^{-2}	...	...
SC&hybrid cell	...	...	...	...	...	2.92%

5. Market availability of solar cells

One of the worlds abundant and clean renewable energy source is solar energy . It is fast growing . Some countries like united states , china ,Spain and Germany have their own largest solar energy harvesting systems. Developed and developing countries across the globe are strongly promoting

solar as an alternative to conventional energy sources and positively influences the solar market .

5.1. PV Market: Global

Solar PV Module Market will growing demand of effective power and large-scale integration of renewable energy. Its Compound Annual Growth Rate (CAGR) of cumulative photovoltaic installations was 35% from years 2010-2019 . According to fraunhofer research PV module production in the year 2019 , China (mainland) hold the lead with a share of 66%, followed by Rest of Asia-Pacific & Central Asia (ROAP/CA) with 18%. Europe contributed with a share of 3%; USA/CAN contributed 4%. Now a days the power demand increases across the commercial establishments including Bitcoin mining devices , hotels, schools & colleges and resorts . This demand pressures toward decentralized power generation will escalate the solar PV module industry.

In the future, the global market for Solar Cells & Modules is projected to reach US $136.5 billion by the year 2027 driven by a post COVID-19 cause of 6.5% over the analysis period 2020 through 2027. In the following fig . 5.1a shows PV Module Production by Region and helps us which country produces more solar cell. [Reference 101]

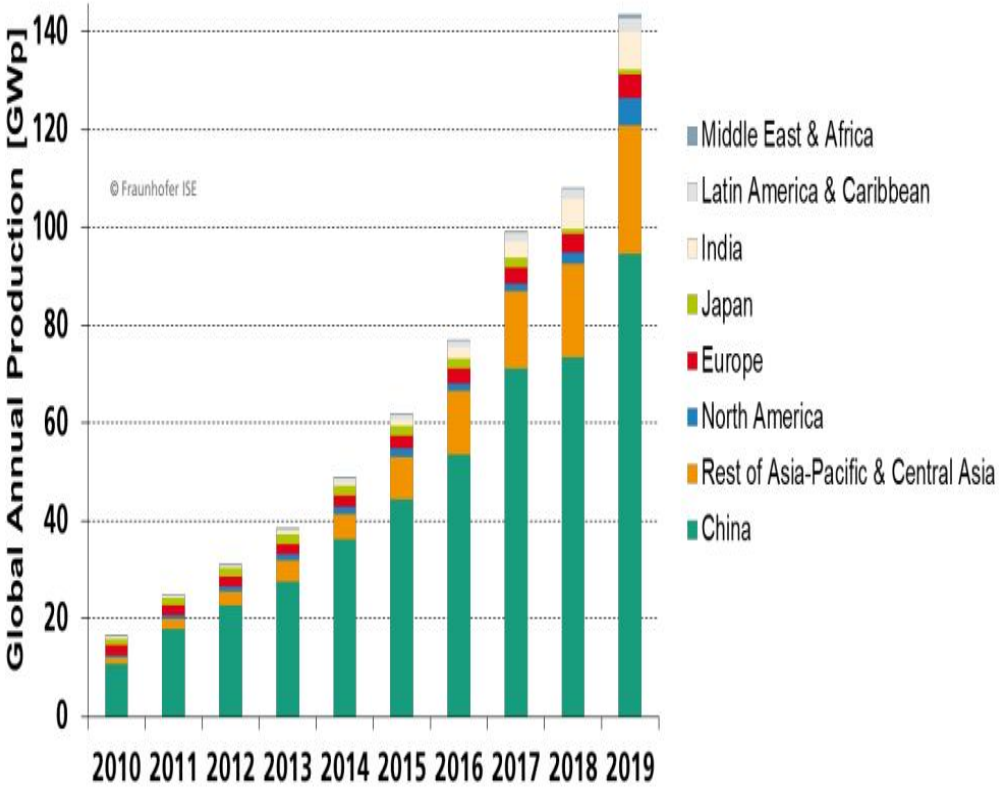

5.2 . The effect of COVID-19 on PV Market

In 2020 , COVID-19 affects the pv market and its production in renewable solar industry . Here are the major things that affect its production.

a. The imports of row materials towards the industry is halt and unable to distribute the products towards other countries due to lock down (PV modules, support structures, etc.).

b. Delay of projects due to cancelation of meetings and negotiations

c. Shortage of workers at installation sites

d. Delay of financing

e. Shortage of workers for manufacturing and other reasons . More detailed can be seen on the figures of section 6.

6. Industries which commercialized solar cells and super capacitors

6.1 . solar cell commercializing industries

According to the recent report , the top 10 manufacturers and suppliers of solar cells are revised in the following table . It compares the 3 years of shipment .

Rank	1H 2020 Shipment preliminary (GW)		2019 Shipment pleriminary (GW)		2018 Shipment (GW)	
1	JinkoSolar (China/ Malaysia/ USA)	8	JinkoSolar (China/ Malaysia/ USA)	14.3	JinkoSolar(China/Malaysia)	11.17
2	LONGi Green Energy Technology (China/ Malaysia)	6.8	JA Solar Technology (China/ Malaysia/ Vietnam)	10.3	JA Solar(China/Malaysia)	8.5
3	Trina Solar (China/ Thailand)	5.84	Trina Solar (China/ Thailand)	10	Trina Solar(China/Thailand)	7.54
4	JA Solar Technology (China/ Malaysia/ Vietnam)	5.46	Canadian Solar (Canada/ China/ Brazil/ Vietnam/ Taiwan)	8.6	Canadian Solar (Canada/China/Brazil/Vietnam)	6.82
5	Canadian Solar (Canada/ China/ Brazil/ Vietnam/ Taiwan)	5.12	LONGi Green Energy Technology (China/ Malaysia)	8.4	LONGi Green Energy Technology (China/Malaysia)	6.58
6	Hanwha Solutions (S. Korea/ China/ Malaysia/ USA)	4	Hanwha Solutions (S. Korea/ China/ Malaysia/ USA)	7.3	Hanwha Q CELLS (S. Korea/China/Malaysia)	5.60
6	Risen Energy (China/ Mexico)	3.37	Risen Energy (China/ Mexico)	6.3	GCL System Integration Technology (GCLSI) (China)	4.57
8	First Solar (USA/ Malaysia/ Vietnam)	2.5	First Solar (USA/ Malaysia/ Vietnam)	5.4	Risen Energy(China)	3.35
8	Zhejiang Chint Electrics (Astronergy) (China)	2.22	Zhejiang Chint Electrics (Astronergy) (China)	3.7	Shunfeng International Clean Energy/Suntech Power(China)	3.30
10	GCL System Integration Technology (GCLSI) (China/ Vietnam)	2	GCL System Integration Technology (GCLSI) (China/ Vietnam)	3.6	Chint Electrics(China)	3.15

Table 6.1 PV module top 10 suppliers in 2020 and major manufacturing sites [Reference 100]

From the table , it is clear that in 2020 the shipment is decreased due to covid-19.

6.2 . Supercapacitors commercializing industries

Some of the commercially available supercapacitors are listed below in the table. The data is collected from the manufacturing industries and it contains the characteristics of the supercapacitor.

Manufacturer	Voltage (V)	Capacitance (F)
APowerCap	2.70	55
APowerCap	2.70	450
Asahi Glass	2.70	1375
BatScap	2.70	2680
Fuji	3.80	1800
Ioxus	2.70	3000
Ioxus	2.70	2000
JSR Micro	3.80	1100
JSR Micro	3.80	2300
LS Mtron	2.80	3200
Maxwell	2.70	2885
Maxwell	2.70	605
NessCap	2.70	1800
NessCap	2.70	3640
NessCap	2.70	3160
Panasonic	2.30	0.10
Panasonic	5.50	50
PowerStor	2.50	2.20
PowerStor	16.20	65
Skeleton	3.40	3200
Skeleton	3.40	850
VinaTech	2.70	336
VinaTech	3.00	342
Yunasko	2.70	510
Yunasko	2.75	480
Yunasko	2.75	1275
Yunasko	2.70	7200
Yunasko	2.70	5200

Table 6.2 a. Commercially available supercapacitor (SC) [Reference 98]

According to Thomasnet.com company profiles of super capacitors the top 12 global EDLC manufacturers are listed below in alphabetical order. It contains start up , manufacturer is headquarter and some of the estimated financing for start up & revenue dollar is not included in data .

	Company	Country	Founded	Estimated Financing*	Revenue**
1	Cellergy	USA	2002	NA	NA
2	Ioxus	USA	2007	$160.1 Million	NA
3	Maxwell Technologies	USA	1965	NA	$130.4 Million
4	Murata Manufacturing	Japan	1944	NA	NA
5	Nanoramic Laboratories	USA	2008	$9 Million	NA
6	Nec Tokin	Japan	1938	NA	$24.0 Billion
7	Nippon Chemi-Con	Japan	1931	NA	$1.02 Billion
8	Panasonic	Japan		NA	$71.8 Billion
9	Paper Battery Company	USA	2008	$5.7 Million	NA
10	Skeleton Technologies	Estonia	2009	$53.8 Million	NA
11	Yunasko	UK	2010	NA	NA

Table 6.2 b. top 12 global EDLC manufacturers . [Reference 103]

Note :- The financing date report is August 8, 2018 and converted to US dollars using foreign exchange rates as of August 9, 2018.

The revenue is reported as of 2017 and converted to US dollars using foreign exchange rates as of August 9, 2018.

7. SWOT analysis of solar cells and super capacitors

SWOT analysis is a methodology that evaluate the internal and external factors of a company to analyse the internal factor which is the advantage (Strengths) or deficiencies (Weaknesses) and the external attributes of the company which touches Opportunities or that cause trouble (Threats) . So the analysis is important for evaluation prioritized based on their significance to the strategic objectives.

7.1 . SWOT analysis solar cells

A. Strength

(i). Limitless :- Solar energy is one of unlimited free energy on the earth and it can fulfil the energy demand of the world . Its approximated energy annually reaching on the earth surface is 4200 times the energy that human population

will consume in the year 2035. So this indicates that solar energy could potentially solve the energy demand of the world without requiring additional sources of energies .

(ii). Environmental Friendly :- It reduces the release of carbon dioxide or harmful gases to the environment that comes out from different generators .

(iii) . Ease of usage/harvest :- The installation of the solar panel can be implemented any where like rooftops, windows , doors or any other places that the sun light reaches.

(iv). Less overall cost :- Once the Solar panels is installed , it required less maintenance cost and cost and can work for 10 to 15 years .

(v). Versatile :- solar cells can be used directly or indirectly in many application that requires electricity .

B. Weakness

(i) . Solar Power is Available Only in Day Time :- The solar panel works only on the day because the sunlight availability . So to get uninterrupted power supply it needs storage devices like batteries and it needs extra cost .

(ii). Solar Panels are inefficient:- Due to inefficiency of the panels , large spaces are required to collect solar energy which is enough for an average household .

(iii) . High Initial Cost :- The initial cost is depends on the assistance of the manufacturing company and the tax of the governments.

C. Opportunities

(i) . Create New Business Opportunities :-The demand of solar energy is increasing and manufacturing industries increasing their products every year . For this reason landowners get a good opportunity to rent their lands for solar farms and they get income .

(ii). Availability of Subsidy and Support :- countries like Malaysia , the government supports individuals and companies which use solar PV as energy sources instead of the conventional fuels.

(iii) . Cost Reduction:- Now adays the completion of the technology results in an improved efficiency and cost reduction. For example silicon photovoltaic cells has dropped dramatically in the past years as shown in the fig.7.1 below.

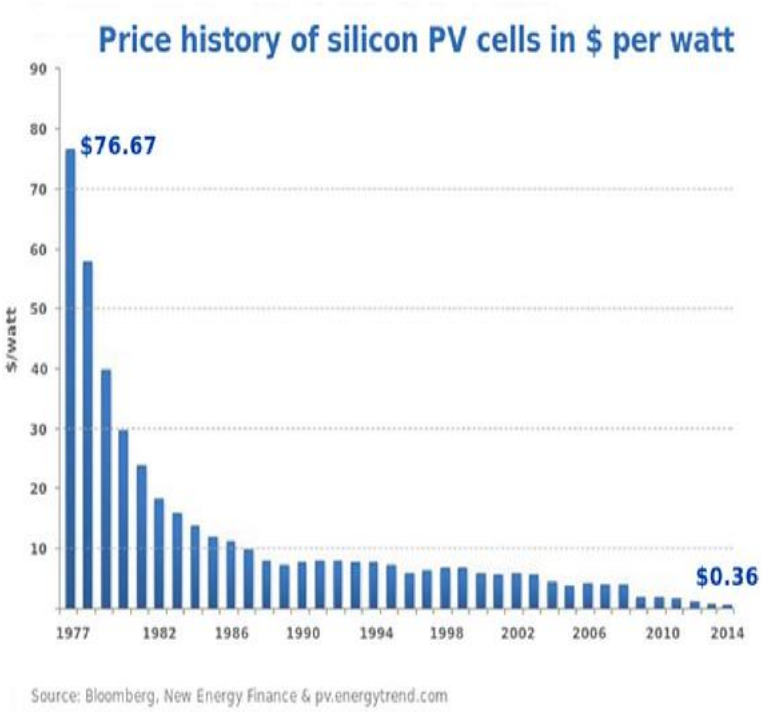

fig.7.1. Cost of silicon photovoltaic cell over the last few decades [Reference 99]

D. Threats

One of the cleanest energy source in the world is solar energy but there is some sort of risk to the environment .

(i). Health risks:- Some countries like china and India burn the waste of some solar panels or e-waste to reclaim the copper wires . The smoke contains poisonous vapor that may cause cancer and teratogenic (birth deformity) when it's being inhaled.

(ii). High carbon footprint:- It can be characterized by the total amount of greenhouse gases produced to either directly or indirectly in the process of realization of a product. For example Concentrated Solar Power (CSP) has an impression of 20 grams of carbon dioxide (CO_2) per kilowatt-hour (kWh) of power delivered.

7.2 . SWOT analysis supercapacitors

The mechanism of storing electrical energy in supercapacitor is by applying DC voltage between two electrodes and their operation principle is not new . The improved technology of supercapacitors uses modern materials that have higher dielectric constants to providing much higher energy storage capacity.

a. Strengths

(i). One of the interesting part of super capacitor is fast charge and discharge rates . Due to this reason supercapacitors are safe.

(ii). The life cycle of charge -discharge is infinite and there is no need to repair them.

(iii). Supercapacitors are friendly to the environment .

b. Weaknesses

(i). The DC voltage of the supercapacitor needs converter which affects the efficiency and cost.

(ii). The cost of supercapacitors is high.

c. Opportunities

(i). Supercapacitors be recharged much faster than batteries.

(ii). supercapacitors have lower weight and a longer lifetime.

(iii). Supercapacitors can advantageously replace batteries in some applications.

d. Threats

Some technologies are mature and cost-effective than supercapacitors. So supercapacitors are applied utility-side of energy storage

8. FUTURE POSSIBLE DEVELOPMENTS

The most needed solar cells for the future are flexible and wearable integrated devices due to light weight, shatter-resistant and they exhibit high specific power. The technology of flexible solar cells is also reposed on the flexible substrates, for instance: the stainless steel or polymers. As most of the solar cells have requirements of high transparency of the electrodes, researchers are searching for flexible transparent materials to replace the hard glasses in the part of light blocking layer. The flexible structure of solar cells provides opportunities to continuous and mass production of power supply in the future. Finally, for the storage part of the supercapacitor which is the photo-charge electrode materials needs some improvements having high capacitances when integrating with the photo harvesting devices like dye-

sensitised, organic, perovskite and soon. (Section 4.1). In recent experiments showed that ultra-supercapacitors can be applicable for the future power bank for small devices. Future explorations should be aimed at optimizing the device parameters for both energy harvesting devices and the storage devices with different material integration and compatibility for better performance . The recent research summarized some materials for both wearable energy harvesting devices and wearable energy storage devices which is shown below in the table 1 and 2

[Reference 5]

Classification	Materials	V_{oc} [V]	J_{sc} [mA cm^{-2}]	FF	Efficiency [%]
DSSC	TCO free TiO_2 film	0.707	5.07	0.676	2.4
	Oriented, crystalline ZnO nanowire array	0.61–0.71	5.3–5.85	0.36–0.38	1.2–1.5
	TiO_2 nanowire array	–	–	–	5.38
	TiO_2 nanotube array	0.670	15.46	0.648	6.72
	TiO_2 nanocrystal film	–	–	–	7.19
	TiO_2 micro cone array	0.702	16.036	0.717	8.07
	Hydrophilic and hydrophobic CNT	0.725	19.43	0.71	10.00
Fiber shaped polymer solar cell	Conducting polymer	0.607	11.9	53.8	3.87
	Polystyrene templated TiO_2 nanocrystalline film	0.36	6.49	0.58	1.38
	P3HT:PCBM and PEDOT:PSS layers	–	–	–	1.08 and less than 3% variation after 200 bending cycles
Fiber shaped perovskite solar cell	Perovskite $CH_3NH_3PbI_3$	0.664	10.2	0.487	3.3 and 95% PCE retained after 50 bending cycles
	Perovskite nanocrystals on CNT fiber	0.615	8.75	0.564	3.03 and 89% PCE retained after 1000 cycles
	Ti/c-TiO_2/meso-TiO_2/perovskite/spiro-OMeTAD/Au	0.713	12.32	0.609	5.35
	Perovskite on CNT sheet	0.85	14.5	0.56	7.1
	Perovskite on TiO_2	0.87	14.18	0.61	7.53

Table 1. Performance of wearable energy harvesting devices.

Classification	Active material	Performance
Lithium-ion battery (LIB)	Ni–Sn and $LiCoO_2$	Cell capacity: 1 mA h cm^{-1}; Output voltage: 3.5 V
	CNT/silicon//CNT/$LiMn_2O_4$	Specific capacity: 106.5 mA h g^{-1}; Voltage output: 3.4 V; Linear energy density: 0.75 mW h cm^{-1}; Areal energy density: 4.5 mW h cm^{-2}
	CNT/$Li_4Ti_5O_{12}$//CNT/$LiMn_2O_4$	Energy density: 17.7 mW h cm^{-3}; Power density: 0.56 W cm^{-3}; Capacity retention: 97% after 1000 bending cycles, 84% after 200 stretching cycles
	$Li_4Ti_5O_{12}$//$LiFePO_4$	Specific capacity: ≈98 mA h g^{-1}; Capacity retention: 91.8% after 40 cycles equivalent to 5500 deep folding–unfolding cycles
	$Li_4Ti_5O_{12}$//$LiCoO_2$	Maintains capacity density: ≈1.1 mA h cm^{-2}; Output voltage: 2.5 V; reversible stretchability: 300%
	MWCNT/$Li_4Ti_5O_{12}$//MWCNT/$LiMn_2O_4$	Specific capacity: 91.3 mA h g^{-1}; capacity retention: 88% after 600% stretching
	CNT/$Li_4Ti_5O_{12}$//CNT/$LiMn_2O_4$	Specific capacity: 92.4 mA h g^{-1}; capacity retention: 92.1% after 100 cycles, 99% after 300 stretching cycles
	CNT/$LiFePO_4$//CNT/$Li_4Ti_5O_{12}$	Specific capacity: 110 mA h g^{-1}
Yarn supercapacitor	CNT@PANI	Areal capacitance: 38 mF cm^{-2} at 0.01 mA cm^{-2}; maintaining almost full capacitance after 150 bending cycles
	IR-CNT@PEDOT/PSS	Specific capacitance: 18.5 F g^{-1} at 0.1 A g^{-1}; Retained 98.8% of capacitance after 200 bending cycles
	CNT/MnO_2	Specific capacitance: 12.5 F g^{-1} at 0.14 A g^{-1}; retained 99.5% capacitance after 200 bending cycles. 42.0 W h kg^{-1} at a lower power density of 483.7 W kg^{-1}, and 28.02 W h kg^{-1} at a higher power density of 19.250 kW kg^{-1}
	Pt/CNT/PANI	Specific capacitance: 86.2 F g^{-1} at 5 mV s^{-1}; energy density of 35.27 W h Kg^{-1} and power density of 10.69 kW Kg^{-1} at 100 mV s^{-1}
	1. PtCu + CNT	1. Specific capacitance: 148 F g^{-1} at 10 mV s^{-1}
	2. Cu + CNT	2. Specific capacitance: 156 F g^{-1} at 10 mV s^{-1}; 97.5% capacitance retention after 1000 fold/unfold cycles

Fiber/cable supercapacitor	Graphene fibers@3D-G	Areal capacitance: 1.2-1.7 mF cm^{-2}; energy density: 0.4–1.7 × 10^{-7} W h cm^{-2}; power density: 6–100 × 10^{-6} W cm^{-2}
	MnO_2 on ZnO nanowires	Areal capacitance: 2.4 mF cm^{-2} at 100 mV s^{-1}; energy density of 2.7 × 10^{-8} Wh cm^{-2} and power density of 1.4 × 10^{-5} W cm^{-2}
	Commercial pen ink	Areal capacitance: 11.9–19.5 mF cm^{-2}; energy density: 1.76 × 10^{-6}–2.7 × 10^{-6} W h cm^{-2} and a power density: 9.07 mW cm^{-2}
	CuO@AuPd@MnO_2 core–shell NWs	Specific capacitance: 1376 F g^{-1} at 5 mV s^{-1}; 99% capacitance retention after 5000 cycles; 93.4% capacitance retention after 100 bending cycles. Power density: 0.55 mW h cm^{-3} and energy density: 413 mW cm^{-3}
	β-$Ni(OH)_2$//AC	Specific capacitance: 481 F g^{-1} at 5 mV s^{-1}; ASC device: 43.5 F g^{-1} at 5 mV s^{-1}; 76% capacitance retention after 2000 cycles; energy density of 10.7 mW h cm^{-1} at a power density of 169 mW cm^{-1}
	NiO NSs@CNTs@CuO NWAs/Cu//AC@CF	Specific capacitance: 93.42 F g^{-1}; 83.6% capacitance retention after 2000 cycles; energy density of 26.32 W h Kg^{-1} at power density of 1218.33 W Kg^{-1}
	PPy–MnO_2–CNT	Areal capacitance: 1.49 F cm^{-2} at 1 mV s^{-1}; 87% capacitance retention after 2000 cycles; High areal energy density of 33 µW h cm^{-2} at 0.67 mW cm^{-2} and a high areal power density of 13 mW cm^{-2} at 14.7 µW h cm^{-2}
	Fe_2O_3@carbon//MnO2@CuO	Volumetric capacitance: 2.46 F cm^{-3} at 0.13 A cm^{-3}; Good rate capability (95.4%); 98.5% capacitance retention after 200 bending cycles; Energy density of 0.85 mW h cm^{-3} at power density of 0.10 W cm^{-3}
Screen printed supercapacitor	AC (YP17)	Specific capacitance: 85 F g^{-1} at ≈0.25 A g^{-1} in polyester microfiber and cotton lawn; 0.43 mF cm^{-2} at 5 mA cm^{-2} for both fabrics; 92% capacitance retention after 10 000 cycles
	AC (YP17)	Areal capacitance: 0.51 F cm^{-2} at mV s^{-1} and 88 F g^{-1} at 10 mV s^{-1} for knitted CF; 80% capacitance retained after 200 cycles
	FeOOH/MnO_2	Specific capacitance: 350.2 F g^{-1} at 0.5 A g^{-1}; Good rate capability: 159.5 F g^{-1} at 20 A g^{-1}; 95.6% capacitance retention after 10000 cycles

Table 2. Performance of wearable energy storage devices

9. The maximum efficiencies recorded in this report

Type of solar cell according to their class	Description	Power conversion Efficiency(PCE) %
Organic dyes	Using co-sensitizer LEG4 (a carboxy-anchor organic sensitizing dye) by replacing metal by organic dyes.	14.3
Photosensitizer Dyes	D–π-A , Adeka-1 + LEG4, Cobalt-based electrolyte:[Co2+(phen)3](PF6^{-})2	14.3
Flexible DSC	2 percent of carbon nanotubes(CNT) in the CNTs/TiO2/C different element	3.38
Wearable DSC	By using TiO_2 layer /Ti wire as a Photoanode and Pt wire as Counter electrode	6

carbon counter electrodes based perovskite solar cells (PSCs)	With FTO/c-TiO2/m-TiO2/perovskite/HTL/carbon configuration and Solvent exchange modification technique	19.2

10. COMMENTS AND CONCLUSIONS

Various flexible /wire-shaped solar cells have achieved for great progress in recent years and their energy conversion efficiency is increasing more than 3%. Moreover, ultra-long, flexible, stable and lightweight devices have been reported as potential flexible/wearable power sources. However, these notable features were realized in different systems. For example, high efficiencies appeared without long-term stability and large size. Lightweight and stable devices were reported with relatively low efficiency or power output. Some recent literatures report that perovskite solar cells, which can be constructed via solution process, can be a suitable candidate for efficient solid photovoltaic fibers. Further material science, interface engineering and structural designs can promote perovskite solar fibers to higher levels, such as efficient perovskite solar wires in tens of centimetres, self-standing devices with harmless/protective packages and solar textiles for wearable power sources. Beyond material science and fiber architectures other considerations such as technical solutions to controllable electrode disposition and efficient manufacture/integration may be considered for actual solar textiles. The structure of fiber devices has also been extensively developed to flexible or even elastic 3D solar devices and integrated energy systems for wearable devices.

11. Acknowledgement

I would like to express my gratitude first to my supervisor Professor Elena Tresso, who guided me throughout this research thesis, Nanomaterials and nanotechnologies for energy applications laboratory guiding professors & assistants , all professors of NANOTECHNOLOGIES FOR ICTs , all class mates and my friends who supported me directly and indirectly.

12. References

[1] . M . Mujahid , C . Chen , W . Hu , Z-K . Wang and Y . Duan , '' Progress of High-Throughput and Low-Cost Flexible Perovskite Solar Cells'' , Sol. RRL , 2020, 4, 1900556

[2]. B. Jinisha , K. M. Anilkumar , M. Manoj ,C . M . Ashraf , V. S. Pradeep and & S. Jayalekshmi , '' Solid-state supercapacitor with impressive performance characteristics, assembled using redox-mediated gel polymer electrolyte'' , J .Solid State Electro .chem , 2019 , 23 , 3343–3353

[3] . S . Iwata , S-I . Shibakawa , N . Imawaka and K . Yoshino , '' Stability of the current characteristics of dye-sensitized solar cells in the second quadrant of the current–voltage characteristics'' , sci. dir. , 2018 , 4, 8-12

[4] . B. Hussain and A. Ebong , '' Specifications of ZnO growth for heterostructure solar cell and PC1D based simulations'' , Elsevier Inc. ,2015 , 5 , 516–521

[5]. S.J. Varma, K. S. Kumar, S.Seal, S. Rajaraman and J. Thomas, '' Fiber-

Type Solar Cells, Nanogenerators, Batteries and Supercapacitors for Wearable Applications '', Adv.Sci, 2018, 5, 1800340

[6]. P . Sundriyal and S . Bhattacharya , '' textile-based supercapacitors for fexible and wearable electronic applications'' , Sci. Rep. , 2020 , 10, 13259

[7]. L. Song , P. Chen , Z. Li , P. Du , Y. Yang , N . Li and J . Xiong , '' Flexible carbon nanotubes/TiO2/C nanofibrous film as counter electrode Of flexible quasi-solid dye-sensitized solar cells'' , Sci.Direct, 2020, 711, 138307

[8]. J . Liu , Y . Li , S . Yong , S . Arumugam and S . Beeby , '' Flexible printed Monolithic structured solid-state Dye sensitized solar Cells on Woven Glass Fibre textile for Wearable energy Harvesting Applications'' , Sci.Rep. , 2019 , 9 ,1362

[9] . A.A .Arbab, M. Ali ,A.A. Memon, A.C. Sun , B.J. Choi and S.H. Jeong , '' An all carbon dye sensitized solar cell: A sustainable and low-cost Design for metal free wearable solar cell devices'' , Elsevier, 2020 , 569 , 386– 401

[10] . H . Baig , H. Kanda , A. M. Asiri , M .k. Nazeeruddin and T. Mallick , '' Increasing efficiency of perovskite solar cells using low concentrating photovoltaic systems'' Sustainable Energy Fuels,2020,4,528

[11] . M. Wu , M , Sun , H . Zhou , J-Y . Ma and T . Ma , '' Carbon Counter

Electrodes in Dye-Sensitized and Perovskite Solar Cells'' , Adv. Funct. Mater. , 2020, 30, 1906451

[12] . N .Jamalullail , I .Smohamad , M .Nnorizan and N . Mahmed , '' Enhancement of Energy Conversion Efficiency for Dye Sensitized Solar Cell Using Zinc Oxide Photoanode'' , Mater. Sci. Eng., 2018, 374 ,012048

[13] . Dr. L. Huang, Prof. Dr. L. Dai , Dr. D. Santiago and Dr. P. Loyselle , '' Graphene-Based Nanomaterials for Flexible and Wearable Supercapacitors'' , WILEY-VCH, DOI: 10.1002

[14]. Y . Wang ,W .Huo , X . Yuan and Y . Zhang , '' Composite of Manganese Dioxide and Two-dimensional Materials Applied to Supercapacitors'' , Acta Phys. -Chim. Sin., 2020, 36(2), 1904007

[15] . Y . Xie , Y . Liu , Y . Zhao , Y. H. Tsang , S. P. Lau , H . Huang and Y . Chai , '' Stretchable all-solid-state supercapacitor with wavy shaped polyaniline/graphene electrode'' , J. Mater. Chem. A,2014,2,9142

[16] . W. K. Chee , H. N. Lim , Z. Zainal , N. M. Huangs, I. Harrison and Y. Andou , ''Flexible Graphene-Based Supercapacitors'' J. Phys. Chem. C 2016, 120, 8, 4153–4172

[17] . S . J . Varma , K . S . Kumar , S . Seal , S . Rajaraman and J . Thomas , '' Fiber-Type Solar Cells, Nanogenerators, Batteries, and Supercapacitors for Wearable Applications'' , Adv. Sci. , 2018 , 5(9) , 1800340

[18] . V . V . Garita , L . R . Elizondo , N . Narayan and P . Bauer , '' Integrating a photovoltaic storage system in one device: A critical review '' , Prog

Photo volt Res Appl. , 2019 , 27 , 346–370

[19]. S . Yun , Y . Zhang , Q .Xu , J .Liu and J. Qin , '' Recent advance in new-generation integrated devices for energy harvesting and storage'' , Sci.Direct , 2020 , 60, 600–619

[20] . M. Yassine and D . Fabris ,'' Performance of Commercially Available Supercapacitors'' , Energies, 2017, 10, 1340

[21] . J .H. Kim, S. K. Hong, S .J. Yoo, C. Y. Woo, J. W. Choi, D. Lee, J .W. Kang,

H . W . Lee and M . Song , '' Pt-free, Cost-Effective and Efficient Counter Electrode with Carbon Nanotube Yarn For Solid-State Fiber Dye-Sensitized Solar Cells'' , Sci.Direct , 2020 , 185 , 108855

[22] . N. Sangiorgi, A. Sangiorgi , A. Dessì, L. Zani, M. Calamante, G. Reginato,

A. Mordini , A. Sanson ,'' Improving the efficiency of thin-film fiber shaped dye-sensitized solar cells by using organic sensitizers'' , Sci.Direct, 2020 , 204 , 110209

[23] . Y. Wu, C . Li , Z . Tian and J . Sun , '' Solar-driven integrated energy systems: State of the art and challenges'' , Sci.Direct, 2020 , 478 , 228762

[24] . S . Yang , S . Sha , H . Lu , J . Wu , J . Ma , D . Wang and Z. Sheng , '' Electrodeposition of hierarchical zinc oxide nanostructures on metal Meshes as photoanodes for flexible dye-sensitized solar cells'' , Sci.Direct, 2020 , 594 , 124665

[25] . H . Zhang , Y . Lu , W . Han , J . Zhu , Y . Zhang and W . Huang , '' Solar

energy conversion and utilization: Towards the emerging photoelectrochemical devices based on perovskite photovoltaics'' , Sci.Direct, 2020 , 393 , 124766

[26] . J . Choi , D . Kwon , B . Kim , K . Kang , J . Gu , J . Jo , K . Na , J . Ahn , D.D . Orbe , K. Kim , J . Park , J . Shim , J. Y . Lee and I . Park , '' Wearable self-powered pressure sensor by integration of piezo-transmittance microporous elastomer with organic solar cell'' , Sci.Direct, 2020 , 74 , 104749

[27] . M.S. D . Medeiros , D . Chanci and R.V. Martinez , '' Moisture-insensitive, self-powered paper-based flexible electronics'' , Sci.Direct, 2020 , 78 , 105301

[28] . Y . Hu , S . Ding , P . Chen , T . Seaby , J . Hou and L . Wang , '' Flexible solar-rechargeable energy system '' , Sci.Direct, 2020 , 32 , 356–376

[29] . B . Li , X . Liang , G . Li , F . Shao , T . Xia , S . Xu , N . Hu , Y . Su , Z . Yang and Y . Zhang , '' Inkjet-Printed Ultrathin MoS_2-Based Electrodes for Flexible In-Plane

Micro supercapacitors'' , ACS Appl. Mater. Interfaces, 2020, 12, 39444–39454

[30] . J .H . Kim , S-J . Koo , H . Cho , J . W . Choi , S . Y . Ryu , J-W . Kang, S-H . Jin , C . Ahn and M . Song , '' 6.16% Efficiency of Solid-State Fiber Dye-Sensitized Solar Cells Based on LiTFSI Electrolytes with Novel

TEMPOL Derivatives'' , CS Sustainable Chem. Eng. , 2020, 8, 40

[31] . A . S . Ghouri , R . Aslam , M . S . Siddiqui and S. K . Sami, '' Recent Progress in Textile-Based Flexible Supercapacitor'' , Frontiers in Materials , 2020 , 7, 58

[32] . N . Anjum , M . Grota ,D . Li and C . Shen , '' Laminate composite-based highly durable and flexible supercapacitors for wearable energy storage'' , Sci.Direct , 2020 , 29 , 101460

[33] . S .A . Hashemi , S . Ramakrishna and A . G . Aberle , '' Recent progress in flexible–wearable solar cells for self-powered electronic devices'' , Energy Envi.Sci. , 2020, 13, 685—743

[34] . D. Lau , N. Song, C. Hall , Y. Jiang , S. Lim, I. Perez-Wurfl, Z. Ouyang, A. Lennon , '' Hybrid solar energy harvesting and storage devices: The promises and challenges'' ,Sci.Direct , 2020 , 13, 22-44

[35] . Chao Lu and Xi Chen , '' Latest Advances in Flexible Symmetric Supercapacitors: From Material Engineering to Wearable Applications'' , Acc. Chem. Res. , 2020, 53, 1468−1477

[36] . D. Zhou , F . Wang, X . Zhao , J . Yang , H . Lu , L-Y . Lin and L-Z . Fan , '' Self-Chargeable Flexible Solid-State Supercapacitors for Wearable Electronics'' , ACS Appl. Mater. Interfaces , 2020, 12, 40

[37] . Y . Li , Z . Lu , B . Xin , Y . Liu , Y . Cui and Y . Hu , '' All-solid-stateflexible supercapacitor of Carbonized MXene/Cotton fabric for wearable energy storage'' , Sci.Direct , 2020 , 528 , 146975

[38] . C . J . Raj , R . Manikandan , W – J . Cho , K .h . Yu and B.C . Kim , '' High-performance flexible and wearable planar supercapacitor of manganese dioxide nanoflowers on carbon fiber cloth'' , Sci.Direct , 2020 , 46 , 21736–21743

[39] . Z . Wang , M . Zhu , Z . Pei , Q . Xue , H . Li , Y . Huang and C . Zhi , '' Polymers for supercapacitors: Boosting the development of the flexible and wearable energy storage'' , Sci.Direct , 2020 , 139 , 100520

[40] . C.V.V. Muralee Gopi , R. Vinodh , S . Sambasivam , I .M . Obaidat and H. J . Kim , '' Recent progress of advanced energy storage materials for flexible and wearable supercapacitor: From design and development to applications'' , Sci.Direct , 2020 , 27 , 101035

[41] . G . Shan , X . Li and W. Huang , '' AI-Enabled Wearable and Flexible Electronics for Assessing Full Personal Exposures'' , The Innovation , 2020, 1, 100031

[42] . M.R . Benzigar , V.D.B.C . Dasireddy , X . Guan , T. Wu and G . Liu , '' Advances on Emerging Materials for Flexible Supercapacitors: Current Trends and Beyond'' ,Adv. Funct. Mater. , 2020, 10.1002 , 2002993

[43] . D . Chen , K . Jiang , T . Huang and G . Shen , '' Recent Advances in Fiber Supercapacitors: Materials, Device Configurations, and Applications'' , Adv. Mater. , 2020, 32, 1901806

[44] . K . Keum , J .W . Kim , S . Y . Hong , J . G . Son , S-S . Lee and J. S . Ha

, '' Flexible/Stretchable Supercapacitors with Novel Functionality for Wearable Electronics'' , Adv. Mater. , 2020, 2002180

[45] . R . Liu , M . Takakuwa , A . Li , D . Inoue , D . Hashizume , K . Yu , S . Umezu , K . Fukuda and T . Someya , '' An Efficient Ultra-Flexible Photo-Charging System Integrating Organic Photovoltaics and Supercapacitors'' , Adv. Energy Mater. , 2020, 10, 2000523

[46] . Y . Chae and J . Hinestroza , '' Building Circular Economy for Smart Textiles, Smart Clothing and Future Wearables'' , Materials Circular Economy, 2020 , 2 ,2

[47] . N . E . Safie , M . A . Azam , M . F.A. Aziz and M . Ismail , '' Recent progress of graphene-based materials for efficient charge transfer and device performance stability in perovskite solar cells '' , Int J Energy Res., 2020 , 1–28.

[48] . D . Zhang , B . Sun , H . Huang , Y . Gan , Y . Xia , C . Liang , W . Zhang and J . Zhang , '' A Solar-Driven Flexible Electrochromic Supercapacitor'' , Materials, 2020, 13, 1206

[49] . S. K . Chirauri , A. K. Dehury and Y.S . Chaudhary , '' Photo supercapacitors: A perspective of planar and flexible dual functioning devices'' , WIREs Energy Environ. , 2020, e377.

[50] . A . Omar, M . S. Ali and N . A. Rahim , '' Electron transport properties analysis of titanium dioxide dye-sensitized solar cells (TiO2-DSSCs) based natural dyes using electrochemical impedance spectroscopy

concept: A review'' , Sci.Direct , 2020, 207 , 1088–1121

[51] . N . Tomar , A . Agrawal , V . S . Dhaka and P .K . Surolia , '' Ruthenium complexes based dye sensitized solar cells: Fundamentals and research trends'' , Sci.Direct , 2020, 207 , 59–76

[52] . A . Aslam , U . Mehmood , M . Hamza , A . Ishfaq , J . Zaheer , A .u .h . Khan and M . Sufyan , '' Dye-sensitized solar cells (DSSCs) as a potential photovoltaic technology for the self-powered internet of things (IoTs) applications'' , Sci.Direct , 2020, 207 , 874–892

[53] . B . Martin , M . Yang , R . C . Bramante , E . Amerling , G . Gupta , M . F. A .M . van Hest and T . Druffel , '' Fabrication of flexible perovskite solar cells via rapid thermal annealing'' Sci.Direct , 2020, 276 , 128215

[54] . S . Alipoori , S . Mazinani , S .H . Aboutalebi and F . Sharif , '' Review of PVA-based gel polymer electrolytes inflexible solid-state Supercapacitors: Opportunities and challenges'' , Sci.Direct , 2020, 27 , 101072

[55] . R. Perez-Gonzalez , E. Araujo , W.Ge , S. Cherepanov , A. Zakhidov , V. Rodriguez-Gonzalez , A. Encinas and J. Oliva , '' Carbon nanotube anodes decorated with Ag NWs/Ni(OH)2NWs For efficient semi transparent flexible solid state supercapacitors'' , Sci.Direct , 2020, 354 , 136684

[56] . D . K . Shah , Y . H . Son , H . R . Lee , M . S . Lee , C . Y . Kim and O. B . Yang , '' A stable gel electrolyte based on poly butyl acrylate (PBA)-co-

poly acrylonitrile (PAN) for solid-state dye-sensitized solar cells'' , Sci.Direct , 2020, 754 , 137756

[57] . D . Sun , Q . Liu , C . Yi , C . Chen , D . Wang , Y . Wang , X . Liu , M . Li , K . Liu , P . Zhou and G . Sun , '' The construction of sea urchin spines-like polypyrrolearrayson cotton-based fabric electrode viaafacile electro polymerization for high performance flexible solid-state supercapacitors'' , Sci.Direct , 2020, 354 , 136746

[58] . P . Bhargava , W . Liu , M . Pope , T . Tsui and A . Yu , '' Substrate comparison for polypyrrole-graphene based high-performance flexible supercapacitors '' , , Sci.Direct , 2020, 358 , 136846

[59] . S . Liu , L . Wei and H . Wang , '' Review on reliability of supercapacitors in energy storage applications'' , Sci.Direct , 2020, 278 , 115436

[60] . J . G . Krishna , P . K . Ojha , S . Kar , K . Roy and J . Leszczynski , '' Chemometric modeling of power conversion efficiency of organic dyes in dye sensitized solar cells for the future renewable energy'' , Sci.Direct , 2020, 70 , 104537

[61] . N . Kutlu , '' Investigation of electrical values of low-efficiency dye-sensitized solar cells (DSSCs)'' , Sci.Direct , 2020, 199 , 117222

[62] . A .H . Alami , K . Aokal and M . Faraj , '' Investigating nickel foam as photoanode substrate for potential dye-sensitized solar cells applications'' , Sci.Direct , 2020, 211 , 118689

[63] . P . Du , Y . Dong , H . Kang , J . Li , J . Niu and P . Liu , '' Superior cycle stability carbon layer encapsulated polyaniline nanowire core-shell nanoarray free-standing electrode for high performance flexible solid-state supercapacitors'' , Sci.Direct , 2020, 449 , 227477

[64] . S . Zou , X . Liu , Z . Xiao , P . Xie , K . Liu , C . Lv , Y . Yin , Y . Li and Z . Wu , '' Engineering the interface for promoting ionic/electronic transmission of organic flexible supercapacitors with high volumetric energy density'' , , Sci.Direct , 2020, 460 , 228097

[65] . A . Gopalakrishnan and S . Badhulika , '' Effect of self-doped heteroatoms on the performance of biomass-derived carbon for supercapacitor applications'' , Sci.Direct , 2020, 480 , 228830

[66] . Z-E . Chen , Q-L . Qi and H . Zhang , '' Linear donor with multipleflexible chains for dye-sensitized solar cells: Inhibition of dye aggregation and charge recombination'' , Sci.Direct , 2020, 267 , 116473

[67] . M . Hosseinnezhada , K . Gharanjig , M . K . Yazdi , P . Zarrintaj , S . Moradian , M . R . Saeb and F.J . Stadler ,'' Dye-sensitized solar cells based on natural photosensitizers: A green view from Iran'' , Sci.Direct , 2020, , 828 , 154329

[68] . H . A . Maddah , V . Berry and S .K . Behura , '' Biomolecular photosensitizers for dye-sensitized solar cells: Recent developments and critical insights '' , Sci.Direct , 2020, 121 , 109678

[69] . Y . Chen , H . Hu , N . Wang , B . Sun , M . Yao and W . Hu , " Cu(I)/Cu(II) partially substituting the Co(II) of spinel Co3O4nanowires with 3D interconnected architecture on carbon cloth for high-performance flexible solid-state supercapacitors'' , Sci.Direct , 2020, 391 , 123536

[70] . F . Shao , N . Hu , Y . Su , L . Yao , B . Li , C . Zou , G . Li , C . Zhang , H . Li , Z . Yang and Y . Zhang , " on-woven fabric electrodes based on graphene-based fibers for areal energy-Dense flexible solid-state supercapacitors'' , Sci.Direct , 2020, 392 , 123692

[71] . I . K . Moon , B . Ki and J . Oh , '' Three-dimensional porous stretchable supercapacitor with wavy structured PEDOT:PSS/graphene electrode'' , Sci.Direct , 2020, 392 , 123794

[72] . C . Xiong , M . Li , W . Zhao , C . Duan , L . Dai , M . Shen , Y . Xu and Y . Ni , " A smart paper@polyaniline nanofibers incorporated vitrimer bifunctional device with reshaping, shape-memory and self-healing properties applied in high-performance supercapacitors and sensors'' , Sci.Direct , 2020, 396 , 125318

[73] . W . Li , X . Zu , Y . Zeng , L . Zhang , Z . Tang , G . Yi , Z . Chen , W . Lin , X . Lin , H . Zhou , J . Xiao and Y. Deng , '' Mechanically robust 3D hierarchical electrode via one-step electro-code position towards molecular coupling for high-performance flexible supercapacitors'' , Sci.Direct , 2020, 67 , 104275

[74] . F . Li , W . Deng , J . Li , M . Wang , Y . Hu and M . Liu , " Anti-solvent

free fabrication of FA-Based perovskite at low temperature towards to high performance flexible perovskite solar cells'' , Sci.Direct , 2020, 70 , 104505

[75] . A . Aboulouarda , B . Gultekin , M . Can , M . Erol , A . Jouaiti , B . Elhadadi , C . Zafer , S . Demic , '' Dye sensitized solar cells based on titanium dioxide nanoparticles synthesized by flame spray pyrolysis and hydrothermal sol-gel methods: a comparative study on photovoltaic performances'' , Sci.Direct , 2020, 9(2) , 1569–1577

[76] . X . Zhang , M . Gao , L . Tong and K. Cai , '' Polypyrrole/nylon membrane composite film for ultra-flexible all solid supercapacitor'' , Sci.Direct , 2020, 6, 339-347

[77] . R . Jia , G . Shen , F . Qu and D. Chen , '' Flexible on-chip micro-supercapacitors: Efficient power units for wearable electronics'' , Sci.Direct , 2020, 27 , 169–186

[78] . S . Liu , L . Kang , J . Zhang , E . Jung , S . Lee and S.C. Jun , '' Structural engineering and surface modification of MOF-derived cobalt-based hybrid nanosheets for flexible solid-state supercapacitors'' , Sci.Direct , 2020 , 32 , 167–177

[79] . C . Arbizzani , Y . Yu , J . Li , J . Xiao , Y-Y . Xia , Y . Yang , C . Santato , R . Raccichini and S . Passerini , '' Good practice guide for papers on supercapacitors and related hybrid capacitors for the Journal of Power Sources'' , , Sci.Direct , 2020 , 450 , 227636

[80] . T . Yue , R . Hou , X . Liu , K . Qi , Z . Chen , Y . Qiu , X . Guo and B . Y . Xia , '' Hybrid Architecture of a Porous Polypyrrole Scaffold Loaded with Metal–Organic Frameworks for Flexible Solid-State Supercapacitors'' , ACS Appl. Energy Mater. , 2020, XXXX, XXX, XXX–XXX

[81] . J . Nam , J . H . Kim , C . S . Kim , J-D . Kwon and S . Jo , '' Surface Engineering of Low-Temperature Processed Mesoporous TiO2via Oxygen Plasma for Flexible Perovskite Solar Cells'' , ACS Appl. Mater. Interfaces , 2020, 12, 12648–12655

[82] . B . J . Kim , S . L . Kwon , M-C . Kim , Y . U . Jin , D . J . Lee , J . B . Jeon , Y . Yun , M . Choi , G . Boschloo , S . Lee and H. S . Jung , '' High-Efficiency Flexible Perovskite Solar Cells Enabled by an Ultrafast Room-Temperature Reactive Ion Etching Process'' , ACS Appl. Mater. Interfaces , 2020, 12, 7125–7134

[83] . T . Zhu , Y . Yang , X . Yao, Z . Huang , L . Liu , W . Hu and X . Gong , '' Solution-Processed Polymeric Thin Film as the Transparent Electrode for Flexible Perovskite Solar Cells'' , ACS Appl. Mater. Interfaces , 2020, 12, 15456–15463

[84] . S . Jha , S . Mehta , Y . Chen , L . Ma , P . Renner , D. Y . Parkinson and H . Liang , '' Correction to "Design and Synthesis of Lignin-Based Flexible Supercapacitors" '' , ACS Sustainable Chem. Eng. , 2020, 8, 9597–9598

[85] . Z . Wang , L . Zeng , C . Zhang , Y . Lu , S . Qiu , C . Wang , C . Liu , L .

Pan , S . Wu , J . Hu , G . Liang , P . Fan , H-j . Egelhaaf , C . J . Brabec , F . Guo and Y . Mai , '' Rational Interface Design and Morphology Control for Blade-Coating Efficient Flexible Perovskite Solar Cells with a Record Fill Factor of 81%'' , Adv. Funct. Mater. , 2020, 30, 2001240

[86] . D . Kim , S . S . Shin , S . M . Lee , J . S . Cho , J .H . Yun , H . S . Lee and J . H . Park , '' Flexible and Semi-Transparent Ultra-Thin CIGSe Solar Cells Prepared on Ultra-Thin Glass Substrate: A Key to Flexible Bifacial Photovoltaic Applications'' , Adv. Funct. Mater. , 2020, 30, 2001775

[87] . J . v . Vaghasiya , C-C . Mayorga-Martinez , J . Vyskočil , Z . Sofer and M . Pumera , '' Integrated Biomonitoring Sensing with Wearable Asymmetric Supercapacitors Based on Ti3C2MXene and 1T-Phase WS2Nanosheets'' , Adv. Funct. Mater. , 2020, 30, 2003673

[88] . J . Shang , Q . Huang , L . Wang , Y . Yang , P . Li and Z . Zheng , '' Soft Hybrid Scaffold (SHS) Strategy for Realization of Ultrahigh Energy Density of Wearable Aqueous Supercapacitors'' , Adv. Mater. , 2020, 32, 1907088

[89] . M. k . Aslam , Y . Niu and M . Xu , '' MXenes for Non-Lithium-Ion (Na, K, Ca, Mg, and Al) Batteries and Supercapacitors'' , Adv. Energy Mater. , 2020, 2000681

[90] . F . Liu , J . He , X . Liu , Y . Chen , Z . Liu , D . Chen , H . Liu and H . Zhou , '' MoC nanoclusters anchored Ni@N-doped carbon

nanotubes coated on carbon fiber as three-dimensional and multifunctional electrodes for flexible supercapacitor and self-heating device'' , Carbon Ener. , 2020 , 1–13

[91] . Y . Deng , Y . Ji , F . Chen , F . Ren and S . Tan , '' Superior performance of flexible solid-state supercapacitors enabled by ultrafine graphene quantum dot-decorated porous carbon spheres'' , New J. Chem., 2020,44, 13591

[92] . V . Elayappan , V . Murugadoss , Z . Fei , P . J . Dyson and S . Angaiah , '' Influence of Polypyrrole Incorporated Electrospun Poly (vinylidene fluoride-co-hexafluoropropylene) Nanofibrous Composite Membrane Electrolyte on the Photovoltaic Performance of Dye Sensitized Solar Cell'' , Eng. Sci., 2020, 10, 78–84

[93] . R . Wang , M . Yao and Z . Niu , '' Smart supercapacitors from materials to devices '' , InfoMat. , 2020 , 2 , 113–125.

[94] . M . R . Samantaray , A . K . Mondal , G . Murugadoss , S . Pitchaimuthu , S . Das , R . Bahru and M. A ,
''Synergetic Effects of Hybrid Carbon Nanostructured Counter Electrodes for Dye-Sensitized Solar Cells '' , Materials 2020, 13, 2779

[95] . M . Yamaguchi , T . Masuda , K . Araki , D . Sato , K-H . Lee , N . Kojima , T . Takamoto , K . Okumura , A . Satou , K . Yamada , T . Nakado , Y . Zushi , Y . Ohshita
and M . Yamazaki , '' Development of high-efficiency and low-cost solar

cells for PV-powered vehicles application'' , Prog Photovolt Res Appl. , 2020 , 1–10

[96] . M . Chen , H . Fan , Y . Zhang , X . Liang , Q . Chen and X . Xia , '' Coupling PEDOT on Mesoporous Vanadium Nitride Arrays for Advanced Flexible All-Solid-State Supercapacitors'' , Small , 2020, 16, 2003434

[97] . N . Mariotti , M . Bonomo , L . Fagiolari , N . Barbero , C . Gerbaldi , F . Bella and C . Barolo , '' Recent advances in eco-friendly and cost-Effective materials towards sustainable dye-sensitized solar cells'' , Green Chem., 2020,22, 7168-7218

[98] . M. Yassine and D . Fabris ,'' Performance of Commercially Available Supercapacitors'' , Energies, 2017, 10, 1340

[99] . F. M . Guangul and G.T. chala , '' Solar Energy as Renewable Energy Source: SWOT Analysis'' , Res.Gate , 978-1-5386-8046-9/19/$31.00 ©2019 IEEE

[100]. I . KAIZUKA , '' PV Industry Trends '' , PVPS, 2020 ,Deputy Operating Agent Task 1 IEA PVPS/ Principal Analyst, RTS Corporation

[101] . Dr.C. Sharma and Dr.A . Jain , '' SWOT Analysis for Solar PV-Technology '' , Res. Gate , 2017 , 8, 2

[102] . B. Burger , K . Kiefer , C . Kost , S. Nold , S . Philipps , R . Preu , J. Rentsch ,T . Schlegl ,G . Stryi-Hipp ,H . Wirth and W. Warmuth , '' PHOTOVOLTAICS REPORT'' , Fraunhofer , 2020 , Fraunhofer ISE

FHG-SK: ISE-PUBLIC , www.ise.fraunhofer.de

[103] . Thomas publishing company , ''Top USA and International Capacitor Manufacturers and Suppliers'' , https://www.thomasnet.com